Nanoscale Advances

ROYAL SOCIETY OF CHEMISTRY

REVIEW

View Article Online
View Journal | View Issue

Cite this: *Nanoscale Adv.*, 2025, **7**, 7483

Application of nanomaterials in organoid culture and cryopreservation

Wanjuan He, Qinlin Sun, Dan Ge, Yang Liu * and Bingbing Sun *

Organoids are three-dimensional, self-organizing microtissues obtained from stem cells, primary tissues, or patient-derived tumors through *in vitro* culture, which are invaluable models for studying organ development, disease mechanism modelling, drug screening, and regenerative medicine. Nanomaterials, with unique surface properties and excellent biocompatibility, have emerged as powerful tools in biomedical research, particularly in the fields of organoid construction (*e.g.*, microenvironment modulation and advanced engineering cultivation) and cryopreservation (*e.g.*, intracellular delivery, nanowarming, and ice-inhibition). This review comprehensively discusses the recent advancements in nanomaterial-based strategies for organoid fabrication and cryopreservation while addressing their challenges such as biocompatibility, scalability and long-term safety. Finally, we envision the prospects in the development of advanced nanomaterial-based platforms for organoid construction and cryopreservation with higher biocompatibility and standardization.

Received 31st May 2025
Accepted 23rd October 2025

DOI: 10.1039/d5na00534e

rsc.li/nanoscale-advances

1. Introduction

Organoids are micro-organs formed by stem cells (including embryonic stem cells, pluripotent stem cells and adult stem cells), tumor cells or primary patient-derived cells through three-dimensional (3D) *in vitro* culture. These structures closely emulate the complex architecture of native organs and recapitulate their physiological functions.[1] In recent years, organoids have demonstrated significant potential across various applications including disease modeling, drug screening, personalized therapy, and regenerative medicine.[2–4] For example, intestinal organoids have been successfully employed to study the pathogenesis of Crohn's disease.[5] Furthermore, animal studies have shown that transplantation of intestinal organoids facilitates colon repair after injury.[6] Additionally, the FDA has explored the use of hepatic organoid chips to model human food-borne diseases and evaluate their potential as a replacement for animal models in compound toxicity testing.[7]

Compared with traditional two-dimensional (2D) cell models, organoids exhibit high similarity to the *in vivo* microenvironment.[8] However, their generation and maintenance remain challenging due to immature protocols, which often lead to poor microenvironmental regulation and central necrosis.[9] Therefore, the development of new technologies to precisely control organoid development and function is now a key research focus. Nanomaterials offer a novel strategy to address these challenges due to their unique chemical and physical properties, including programmable surface functionalities and biocompatibility. Nanomaterials can optimize the developmental microenvironment in multiple ways. For instance, Abdel *et al.* found that variations in the concentration of magnetic nanomaterials could precisely control the elastic modulus of Matrigel.[10] This property enables Matrigel to adapt to the microenvironmental requirements of organoids at different growth stages, thereby regulating cellular behaviors such as differentiation. Functional nanomaterials such as mesoporous silica nanoparticles can be used to deliver growth factors and other bioactive molecules, enabling dynamic regulation of stem cell differentiation and organoid morphogenesis.[11] By mimicking the natural extracellular matrix (ECM), nanofiber scaffolds significantly enhance cell adhesion and provide essential mechanical support.[12]

Simultaneously, the establishment of a stable and efficient cryopreservation system is critical to ensure a continuous supply of organoids and facilitate their practical application. Nevertheless, the cryopreservation of organoids remains challenging. A primary difficulty is their size, which limits the rapid transfer of heat and mass. Moreover, most traditional cryoprotectants (CPAs) exhibit cytotoxicity. Nanomaterials offer a promising strategy to overcome these challenges. Nanomaterials such as mesoporous silica and graphene oxide (GO) can serve as heterogeneous nucleation sites, reducing the degree of supercooling and inhibiting the formation of ice crystals. Moreover, magnetic nanoparticles (MNPs) enable uniform thawing under an external physical field, which significantly enhances the post-thaw survival rate of organoids, as demonstrated in heart models.[13]

State Key Laboratory of Fine Chemicals, School of Chemical Engineeringand Frontiers Science Center for Smart Materials Oriented Chemical Engineering, Dalian University of Technology, 116024 Dalian, China

Given these unique attributes, nanomaterials have emerged as a key medium for bridging micro-scale cellular behavior and macro-scale tissue function, demonstrating potentials for promoting organoid technology. Herein, we review the current advances and outline the future perspectives of nanomaterials in organoid construction and cryopreservation.

2. Nanomaterial-assisted organoid culture construction

Organoids can be generated from various sources including adult organ-derived cells, stem cells and tumor tissues. Their development is critically dependent on the staged culture conditions that mimic a specific development path. The developmental cycle varies significantly among organoids from different sources. Stem cell-derived organoids undergo a multi-stage process involving cell proliferation, early differentiation, globular structure formation and maturation. In contrast, organoids derived from primary cells or tumors are more dependent on microenvironmental and signaling cues, resulting in a shorter development cycle.[14] Although current technology enables the construction of 3D organoids, several significant challenges remain. For stem cell-derived organoids, an *in vitro* system can hardly simulate the synergistic effect of multiple growth factors present *in vivo*. This often results in deviations in differentiation stage and direction, incomplete cellular maturation, and consequent functional defects.[8] Organoids derived from primary cells and tumor cells often face gradual loss of function and reduced heterogeneity, respectively.[15,16] In addition, different organoid types face several common challenges. These include poor control over size, shape and cell composition, leading to low experimental repeatability.[17] Furthermore, during long-term culture or upon exceeding a critical size, the lack of a vascular network results in internal hypoxia and subsequent necrosis.[18,19] Organoid culture is critically dependent on the ECM. However, commonly used hydrogel scaffolds such as Matrigel have significant limitations including an unclear composition and limited tunability of mechanical properties. These shortcomings prevent them from fully recapitulating the complex physical microenvironment *in vivo*.

Nanomaterials provide a breakthrough strategy for addressing the aforementioned challenges. Specifically, a cell aggregation pattern can be controlled *via* the dynamic magnetic field based on the MNP-assisted 3D suspension culture technology, reducing the structural heterogeneity.[20] By mimicking the native electrophysiological microenvironment, conductive nanofiber scaffolds promote the synapse formation in brain organoids, and thereby address the issue of insufficient maturity in stem cell-derived organoids.[21] The nanofiber scaffolds can simulate the spatial conditions for organoid growth, prevent uncontrolled cellular proliferation, and help maintain the heterogeneity of tumor organoids.[22] Nanomaterials also function as versatile carriers of growth factors to

Table 1 Nanomaterials for organoid culture[a]

Nanomaterials		Organoids	References
ECM properties modification	Nanocellulose hydrogel	Mouse-derived intestinal organoids	23
	Calcium silicate nanowire-containing hydrogel	Mouse-derived intestinal organoids	24
	AuNRs	Human cardiac organoids	25
	Collagen-carbon nanodots	Mouse-derived neural progenitor spheroid	26
	e-SiNWs	Human cardiac organoids	27
	SiNP	Mouse-derived B cell follicle organoid	11
	BFP-1-laden MSNs	Human bone organoid	28
	DNA microbeads	Medaka-derived retinal organoids	29
3D culture	Magnetic iron oxide (Fe_3O_4), AuNPs	Human glioblastoma tumor spheroid	20
	Carbon-encapsulated cobalt MNPs	Mouse-derived breast cancer spheroid and colorectal cancer spheroid	30
	Magnetic iron oxide (FeO_3)	Human MSC spheroid	31
	Fe_3O_4	Human MSC spheroid	32
	Magnetic iron oxide (Fe_3O_4)-encapsulated PLGA microparticles/PLLA-*b*-PEG-folate NPs	Human epidermoid tumor spheroid	33
	Nanoparticle assembly of Fe_2O_3 and Au NPs cross-linked with PLL	Mouse-derived adipose tissue organoids	34
	Nanoparticle assembly of Fe_2O_3 and Au NPs cross-linked with PLL	Pig-derived salivary adenoid organoid	35
		hFOB spheroid	36
		Human pseudo-islets	37
		3D multicellular spheroid composed of human MSCs, human ECs and human HSCs	38
		Human lung spheroid granuloma model	39
		Human prostate cancer cell spheroid	40
Liquid marble	PTFE powder particles	Human pancreatic mini-organoids	41

[a] ECM: Extracellular matrix; AuNRs: Gold nanoribbons; e-SiNWs: Electrically conductive silicon nanowires; SiNPs: Silicon nanoparticles; NPs: Nanoparticles; BFP-1: Bone formation petitude-1; MSNs: Mesoporous silica nanoparticles; MNPs: Magnetic nanoparticles; MSC: Mesenchymal stem cell; PLGA: Poly(lactic-*co*-glycolide); PLLA: Poly(L-lactic acid); PEG: Poly(ethylene glycol); PLL: Poly-L-lysine; hFOB: Human fetal osteoblast; ECs: Endothelial cells; HSCs: Hematopoietic stem cells; PTFE: Polytetrafluoroethylene.

regulate cell behavior and induce vascularization, thereby alleviating common problems such as internal necrosis.[19] Table 1 outlines various nanomaterials used for organoid culture construction.

2.1 Construction and static modulation of the extracellular microenvironment

The ECM is an acellular 3D network of macromolecules, composed of collagens, proteoglycans and other glycoproteins.[42] As a core component of the cellular microenvironment, it not only provides essential physical support for cells and tissues, but also regulates critical processes such as proliferation, differentiation, and apoptosis through cell membrane-mediated signalling pathways.[43] Therefore, the modulation of ECM properties can direct cell orientation and differentiation, influencing their fate and tissue morphology. A major drawback of conventional ECMs such as Matrigel is their poorly defined composition and simplistic mechanical properties. These materials cannot fully simulate the complex *in vivo* physical microenvironment, which ultimately constrains organoid development.[44] Through methods such as directional arrangement, nanomaterials can effectively simulate the natural ECM and modulate the mechanical properties of matrix adhesives, providing new solutions to the above-mentioned problems.

2.1.1 Structural simulation and remodelling of the natural ECM. Nanomaterials, particularly nanofibers, can simulate the topological structure of the natural ECM, providing a biomimetic microenvironment, and support organoid development. By regulating the parameters such as fiber diameter and porosity, nanofibrous scaffolds can directly influence cellular morphology, guide cells to arrange in a predetermined pattern, and promote the formation of complex 3D tissue structures.[12] Antonova *et al.* applied electrospinning technology to fabricate nylon nanofiber scaffolds. These directionally aligned fibrous scaffolds provided topological cues that mimicked the cell–surface interface of the brain ECM, enabling successful generation and cultivation of neurospheres.[45] You *et al.* cultured cardiomyocytes on 2D aligned polycaprolactone (PCL) nanofiber scaffolds and successfully generated cardiac organoids by manual stacking.[46] However, PCL nanofibers are inherently hydrophobic, which leads to poor cell adhesion performance. Beldjilali-Labro adopted PCL nanofibers coated with gold nanoparticles (Au NPs). This modification significantly enhanced the cellular adhesion performance of the scaffold and effectively promoted the continuous differentiation of skeletal muscle tissue (Fig. 1b).[47] In addition to guiding cell morphology, nanofibrous scaffolds exhibit high porosity and a large specific surface area, ensuring the efficient nutrient transport and reducing the risk of central necrosis.

Similarly, the physical properties of nanomaterials, such as hardness and surface topography, are perceived by mechanical stimulation ion channels in cells, leading to the release of signal factors and the expression of related genes.[51,52] In the osteogenic differentiation of mesenchymal stem cells (MSCs) into bone organoids, nano-hydroxyphosphine with slightly lower hardness and greater surface roughness has been shown to induce the expression of genes in a better way, which promotes osteogenesis.[53] Meanwhile, these nanomaterials can reshape the cellular microenvironment by modulating the synthesis and degradation of ECM-related proteins, thereby indirectly influencing the behavior of surrounding cells.[48] Collagen, elastin, and glycosaminoglycans are key components of the natural ECM. Through their synergistic effects, they endow the ECM with diverse biochemical and mechanical properties. Collagen provides the fundamental structural support and mechanical strength for the ECM. Elastin confers elasticity and toughness to tissues, and glycosaminoglycans enhance the buffering capacity of the ECM and regulate permeability through hydration effects. The proportion of these components of the natural ECM varies significantly across different tissues and organs. Carbon nanotubes have been shown to up-regulate type I collagen gene expression, with longer nanotubes demonstrating better effects than the shorter ones.[54] Poly(lactic-*co*-glycolide) (PLGA) nanoparticles can effectively promote the synthesis of elastin.[55] Therefore, during organoid cultivation, the physicochemical properties of nanomaterials can be harnessed to precisely regulate the synthesis and assembly of core ECM proteins. This strategy allows for the simulation of the specific ECM component characteristics of target tissue.

In addition, recent studies have demonstrated that incorporating conductive nanomaterials into the ECM can effectively enhance the electrical conductivity, thereby promoting the maturation of certain organs. In a study by Tan *et al.*, the integration of conductive silicon nanowires (e-SiNWs) into cardiac organoids improved the electrical conduction velocity and synchronous contraction capabilities of cardiomyocytes.[27] Experiments indicated that e-SiNWs enhance electrical coupling between cells by promoting the expression of gap junction proteins. This enhancement consequently improves the electrophysiological integration efficiency of transplanted cardiac organoids into infarcted myocardium. Similarly, carbon nanodot composites have been shown to significantly promote neurite outgrowth in neural progenitor cell spheres and accelerate the electrical physiological maturation of neurons. These findings offer new strategies and open up new possibilities for functional neural network construction.[26]

2.1.2 Directional regulation of cellular signaling cues. Nanomaterials can serve as carriers for targeted delivery of drugs to specific ECM components. They can encapsulate and provide sustained release of bioactive substances such as growth factors. In their study, Zhou *et al.* found that the cell microenvironment was influenced by nanomaterials *via* regulating the synthesis of a variety of ECM-related proteins and extracellular proteases (Fig. 1a).[48] Purwada *et al.* designed a silicate nanoparticle (SiNP) hydrogel scaffold for immune organoid culture.[11] They demonstrated that SiNP enhances the presentation of key signaling molecules required for B cell follicle activation, thereby accelerating B cell development and differentiation. Based on the alginate hydrogel system developed by Luo *et al.*, the researchers supplemented it with mesoporous silica nanoparticles (pep@MSNs) loaded with bone formation peptide-1 (BFP-1).[28] Pep@MSNs provided sustained release of BFP-1, which could induce human MSC osteogenic

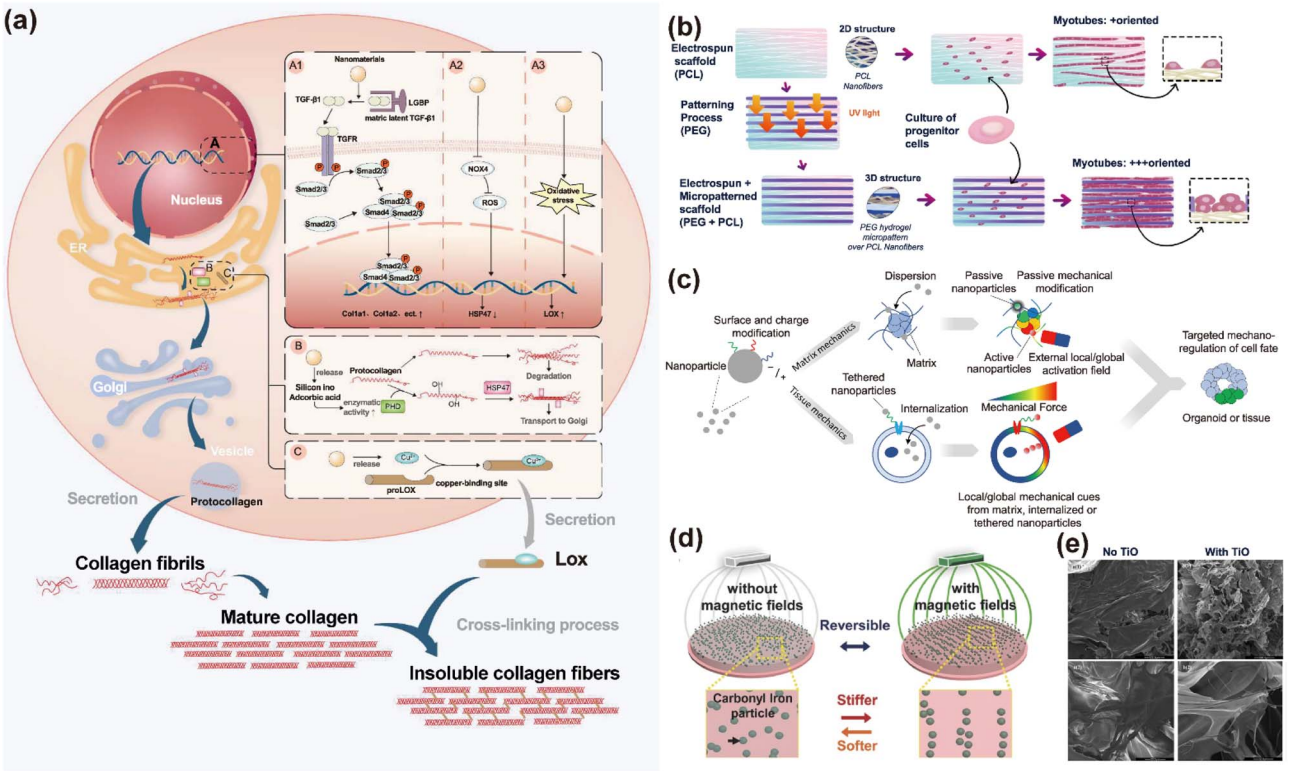

Fig. 1 Role of nanomaterials in regulating the *in vitro* microenvironment. (a) Mechanism by which nanomaterials influence the synthesis and degradation of ECM-related proteins to remodel the cellular microenvironment. (A) Nanomaterials modulate collagen gene expression through multiple pathways. (A1) Activation of the TGF-β/smad pathway. (A2, A3) Transcriptional regulation of HSP47 and lysyl oxidase (LOX) by inhibiting oxidative stress. (B) Nanomaterials facilitate collagen post-translational modification within the endoplasmic reticulum (ER). (C) Nanomaterials modulate extracellular collagen by regulating LOX. This figure has been adapted/reproduced from ref. 48 with permission from the American Chemical Society, copyright 2024. (b) Magnetic nanoparticles (MNPs) can modulate the physical properties of Matrigel through active or passive mechanisms. Under an external magnetic field, activated NPs generate localized mechanical forces, whereas inactive NPs contribute to altering the local matrix stiffness passively. Additionally, magnetized cells experience forces when subjected to an external field and transmit these mechanical stresses to the surrounding extracellular matrix (ECM). This figure has been adapted/reproduced from ref. 47 with permission from Frontiers, copyright 2020. (c) Synthesis and functional schematic of a multiscale scaffold composed of polyethylene glycol and poly(ε-caprolactone) nanofibers for muscle tissue engineering. The aligned nanofibers mimic the nanoscale architecture of the native muscle ECM. This figure has been adapted/reproduced from ref. 10 with permission from MDPI, copyright 2021. (d) In the absence of a magnetic field, the particles remain randomly dispersed, and the hydrogel maintains its soft mechanical properties (left). Under a magnetic field exposure, carbonyl iron particles within the hydrogel align into chain-like structures, resulting in increased stiffness of the material (right). This figure has been adapted/reproduced from ref. 49 with permission from WILEY-VCH Verlag GmbH & Co. KGaA, Weinheim. (e) SEM images of collagen scaffolds before (left) and after (right) the incorporation of titanium oxide nanoparticles. After incorporation, the nanocomposite scaffold changes from a dense, sheet layer-like morphology to a three-dimensional structure with a finer, fluffier fibrous network. This figure has been adapted/reproduced from ref. 50 with permission from Elsevier B.V., copyright 2015.

differentiation following the proliferation stage. Additionally, the peptides were self-captured through an additional cell-cross-linking network, formed by the binding of ligands to cell surface receptors. This mechanism achieved long-term, continuous osteogenic stimulation of hMSCs. This stage-specific and independent controlled sequential stimulation effectively improved the osteogenic capacity of hMSCs, and provides a strategy to stimulate the synergistic effects of multiple factors found *in vivo*.

Afting *et al.* developed nanoscale DNA microbeads for drug delivery. When injected into retinal organoids, these microbeads degrade under ultraviolet physical fields, enabling the gradient release of encapsulated Wnt-surrogate. By adjusting the injection site and photoinitiation parameters, precise spatiotemporal control over organoid development can be achieved, thereby meeting specific mechanical requirements within the organoids.[29]

2.1.3 Adjustment of ECM mechanical characteristics. In the cultivation of organoids, commonly used extracellular matrices such as Matrigel have the problem of single mechanical properties. Although various hydrogels can dynamically modulate stiffness to mimic the tissue development, they typically provide only uniform mechanical cues and cannot recreate the diverse array of local mechanical signals (in both magnitude and direction) that characterize native microenvironments.[56–58] Nanoparticles can provide local or global, passive or active mechanical stress regulation *via* dispersion in the ECM and enable efficient cellular internalization. Compared to NP-free ECM scaffolds,

polyvinylpyrrolidone (PVP)-coated titanium oxide NPs significantly improved scaffold properties and enhanced skin tissue regeneration (Fig. 1e). Bao *et al.* incorporated carbon nanotubes (CNTs) into Matrigel for the culture of intestinal organoids.[59] The results demonstrated that the CNT not only reduced Matrigel hardness but also altered intestinal organoid metabolism, enhancing mitochondrial activity, respiration capacity and nutrient uptake. These synergistic mechanisms collectively promote intestinal organoid proliferation and differentiation, confirming the promising role of nanomaterials in advanced organoid culture systems. Zhang *et al.* reported comparable favorable outcomes by blending $Ti_3C_2T_x$MXenes with Matrigel during culture.[50] Notably, the size of nanomaterials critically determines their modification effects on hydrogels. Smaller nanoparticles can intercalate into the interchain spaces of the hydrogel network, maintaining crosslinking stability while locally increasing rigidity and hardness. In contrast, larger nanomaterials disrupt the cross-linked structure, leading to material softening and reduced stiffness (Fig. 1c).[10]

2.2 Dynamic regulation *via* external physical fields

Nanoparticles can respond to external physical fields and undergo directional movement, aggregation and dispersion behavior changes.[60,61] Thus, active modulation of the physical field enables the precise control of mechanical forces exerted on organoids. This approach enables stage-specific environmental manipulation that closely mimics physiological growth conditions, while offering a simple and versatile platform to meet the distinct mechanical requirements of each organoid developmental phase.[10,62] Simultaneously, the developmental status of organoids can also be monitored in real time by the spatial distribution patterns of MNPs.

2.2.1 Dynamic modulation of extracellular matrix mechanics. Abdeen *et al.* demonstrated that a polyacrylamide hydrogel containing magnetic carbonyl iron (CI) dispersed as particles exhibits field-dependent elasticity modulation.[49] Under an applied magnetic field, nanoparticles will form chain-like structures and accumulate near the magnetic field, locally increasing the scaffold stiffness and resistance to deformation. After removing the magnetic field, the nanoparticles will be dispersed uniformly throughout the scaffold *via* Brownian motion, restoring the original stiffness and mechanical properties. By simple modulation of magnetic field strength, the gel stiffness can be precisely and reversibly tuned, inducing observable biological effects (Fig. 1d). Sapir-Lekhovitser *et al.* similarly applied the same principle to achieve reversible stiffness control in calcium alginate scaffolds.[63] Filippi *et al.* demonstrated that besides the matrix effect, the migrated nanoparticles also interact with cells, thereby stimulating cell metabolic activity.[64] This strategy overcomes the inherent homogeneity of synthetic hydrogels, enabling biomimetic replication of the anisotropic mechanical cues found *in vivo*.

2.2.2 Monitoring and analysis of organoid Developmental Progression. During organoid development, the biological scaffold experiences subtle strain deformation, which induces detectable alterations in the magnetic signals of embedded MNPs. This unique property enables MNPs to serve as imaging agents and biosensors to monitor the dynamic life processes of organoids and deepen researchers control and understanding of organoid development stages. Li *et al.* incorporated ultrasmall superparamagnetic iron oxide (USPIO) nanoparticles into the biological scaffold, which not only improved the mechanical strength of the scaffold, but also enabled the real-time monitoring of bile duct repair and degradation of processes through magnetic resonance imaging (MRI).[65] Zhang *et al.* developed a magnetic hydrogel composed of gelatin methacryloyl/iron oxide (GelMA/Fe_3O_4), which enabled real-time strain monitoring with a sensitivity as high as 50 μm. This innovative approach offers a promising solution for monitoring the culture of cardiac organoids.[66] Ou *et al.* established a wireless biosensor platform by combining an Nd-Fe-B/polydimethylsiloxane (NdFeB/PDMS) magnetic beam structure with aligned PCL nanofibers for myocardial tissue culture.[67] The system enables multidimensional magnetic field analysis for real-time and *in situ* measurement of myocardial tissue contraction forces, demonstrating exceptional sensitivity and repeatability. Lin *et al.* combined the stretchable nanoelectronic networks with 2D cell layers. Leveraging inherent cellular aggregation and other activities, they successfully integrated nano-sensors into 3D organoids.[68] This strategy not only simplified the layer-by-layer cell stacking process but also enabled large-scale, long-term monitoring and stimulation of the organoids.

2.2.3 Three-dimensional (3D) magnetic levitation culture. The magnetic levitation culture represents an emerging 3D culture technology that employs MNPs coupled with magnetic field regulation.[69] This technology involves either surface modification or intracellular incorporation of MNPs into target cells, which then respond to external magnetic force gradients to achieve uniform suspension in a culture medium. This unique configuration promotes spontaneous aggregation, leading to organoid formation. As a representative example, Souza *et al.* established a 3D cell culture platform based on cell MNP-mediated levitation.[20] Cells were co-cultured with a composite hydrogel containing gold nanoparticles, magnetic iron oxide nanoparticles, and filamentous phages. Following cellular uptake of these nanomaterials, the cells acquired magnetic properties and achieved stable suspension in the culture medium. By modulation of the magnetic field parameters, the spatial organization of the cellular assemblies can be engineered, and heterogeneous multicellular aggregation can be achieved. This magnetic manipulation approach effectively improves the reproducibility and uniformity of organoids compared to traditional manual methods. The experimental results showed that the human glioblastoma cells cultured *via* magnetic levitation 3D culture self-assembled into spheroidal tumoroids, which was similar to the *in vivo* human tumor xenograft in the protein expression profile and maintained the invasiveness of the tumor. This technology provides a novel method offering control over both the size and morphology of organoids. Kim *et al.* enhanced the external magnetic field intensity and also achieved the controllable aggregation and fusion of mesenchymal stem cell spheres (Fig. 2a).[70] This

magnetic optimization reduced the cell fusion time and enabled real-time manipulation of cellular organization through field gradients. Tseng *et al.* acquired heterogeneous cell layers by similar techniques and achieved multi-layer tissue constructs. Bronchiolar organoids have been successfully engineered, which advanced complex organoid fabrication.[71]

The internalized NP may accumulate to cytotoxic concentrations, degrade into harmful substances, disrupt cellular morphology and signaling pathways, and ultimately induce necrosis or apoptosis.[72] To mitigate such cytotoxicity, researchers are actively pursuing surface functionalization strategies to improve nanoparticle biocompatibility. Coating nanoparticles with biocompatible materials such as poly-L-lysine or PVP can significantly mitigate cytotoxicity, ensuring normal growth and functionality.[73]

Lee *et al.* successfully engineered human epidermoid tumor spheroids using PLGA particles encapsulated with magnetic iron oxide (Fe_3O_4).[33] The distinction lies in the diameter of the particles: Lee's group utilized larger PLGA particles (20 μm diameter) that remain extracellular throughout the culture process. Instead, cells adhere to the particle surfaces *via* electrostatic interactions, subsequently proliferating to form 3D clusters (Fig. 2e). This design eliminates the possible toxicity risks of nanomaterials. The magnetic field upregulates N-cadherin expression at the cell membranes and junctions, enhancing intracellular interaction and simulating the *in vivo*

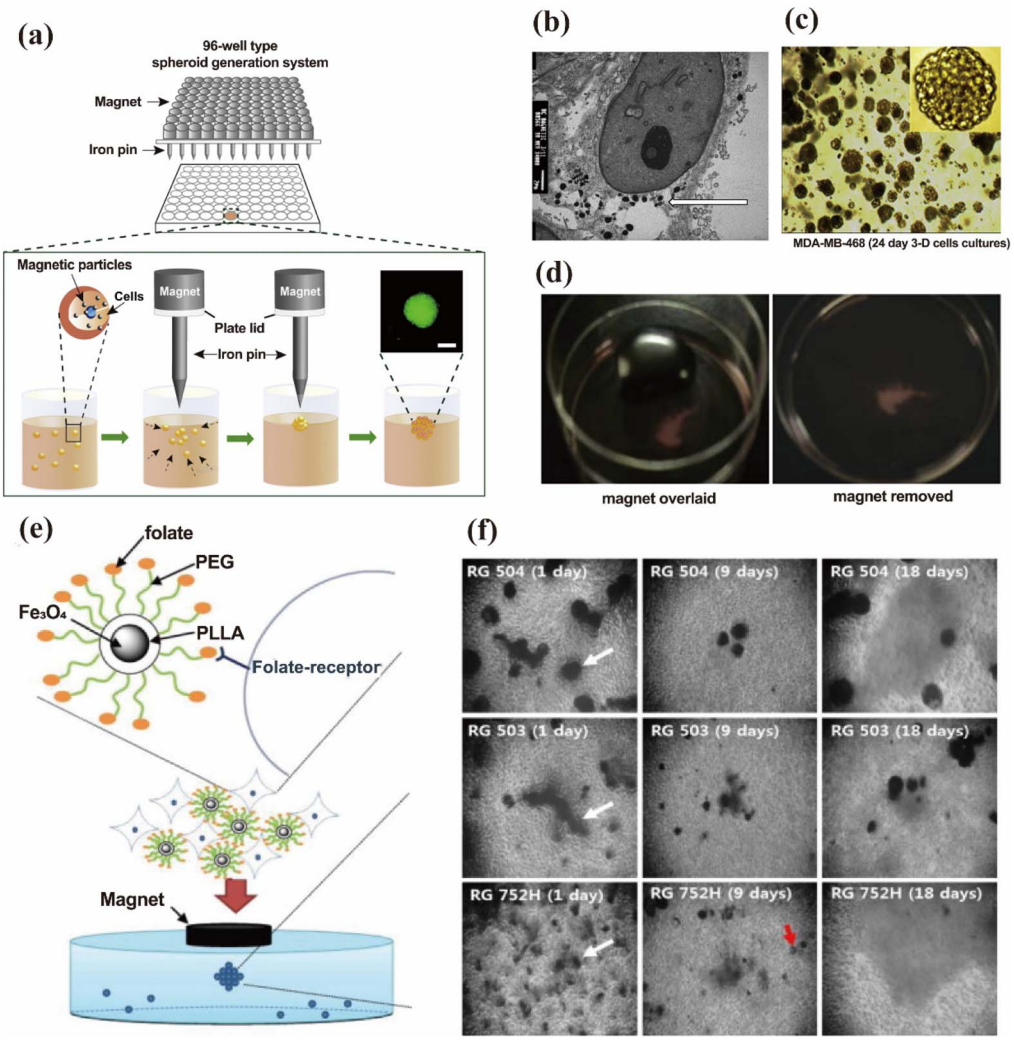

Fig. 2 Magnetic levitation culture for organoid generation. (a) Schematic of the formation of spheroids using magnetic levitation technology. Cells internalize magnetic nanoparticles (MNPs) *via* endocytosis, thereby exhibiting acquired magnetic properties. Under the focused magnetic force from iron pins and magnets, the cells accumulate at specific characteristic positions within the culture medium and gradually assemble into spheroids. This figure has been adapted/reproduced from ref. 70 with permission from Elsevier Ltd, copyright 2013. (b) TEM images of MDA-MB-231 cells containing internalized MNPs. (c) Tumor sphere morphology after 24 days of magnetic suspension culture. (d) Tissue images before and after the removal of the external magnetic field. This figure has been adapted/reproduced from ref. 30 with permission from Elsevier Inc., copyright 2015. (e) Schematic of the magnetic levitation technology mediated by surface adsorption of MNPs. MNPs are bound by electrostatically interacting cell membranes and cultured in a magnetic field for 3D tumor spheroids. (f) Tumor spheroids on different culture days. This figure has been adapted/reproduced from ref. 33 with permission from Elsevier B.V., copyright 2011.

environment. As the PLGA degraded, the magnetic particles were progressively cleansed and cleared, leaving behind the densely packed tumor spheroids (Fig. 2f). Inspired by Lee's work, Rodriguez-Arco synthesized a magnetic nanocomposite with a positively charged core–shell structure, which is designed to bind with negatively charged cell membranes to achieve highly efficient cell magnetization.[74] The core consists of an acrylic monomer copolymer coated with a 10–50 nm layer of iron oxide that provides both magnetic and positive surface charges. Furthermore, the outer surface of the iron oxide layer was modified with a poly(ethylene glycol) (PEG) coating to improve the biocompatibility. Gaitán-Salvatella *et al.* conducted a study on the biocompatibility of a class of nanomaterials that bind to cell membranes *via* electrostatic interactions.[36] The findings demonstrated that these nanomaterials do not interfere with the physiological activities and gene expression of cells; additionally, they are easy to remove, making them suitable for the long-term cultivation of spheroids.

The magnetic levitation culture approach eliminates matrix-induced variability in cell behavior, and the structural diffusion barriers ensure uniform oxygen and nutrient distribution throughout the organoids. Salivary gland organoids cultured *via* magnetic levitation exhibited autonomous ECM deposition, upregulated expression of N-cadherin and epidermal growth factor receptor (EGFR), and stable 3D structures without central necrosis observed in conventional cultures (Fig. 2b–d).[30,35,75]

Several research groups have developed hydrogel-assisted magnetic levitation platforms for improved 3D cell culture formation.[76,77] These platforms have demonstrated successful generation of diverse spheroids and organoids, with more refined spatial organization and natural structure and function.

2.3 Advanced engineering approaches for organoid cultivation

The standardized quality control and high-throughput culture remain critical challenges limiting the large-scale application of organoids, while nanomaterials present promising solutions to these technological barriers. In 3D bioprinting, the rheological properties of nanocomposite bioinks can be precisely tuned by adjusting the concentration and surface modification of nanoparticles, enabling enhanced digital control of printing process. Microbioreactors modified with nanomaterials not only simulate key aspects of the *in vivo* physiological microenvironment but also ensure the uniformity of conditions during organoid growth, thereby facilitating high-throughput organoid production.

2.3.1 Nanoparticle-incorporated 3D bioprinting. Nanomaterial-mediated ECM modification strategies have been adapted for 3D bioprinting, allowing for tunable mechanical and biochemical scaffold properties. Krontiras *et al.* fabricated porous biocomposite scaffolds using bacterial nanocellulose and alginate, demonstrating successful adipogenic differentiation of mouse MSCs on both 2D and 3D scaffolds.[78] Based on this investigation, Markstedt *et al.* formulated a nanofibrous cellulose (NFC)/alginate hybrid bioink for 3D bioprinting of human chondrocytes and cartilage tissue constructs.[79] By adjusting the ratio of NFC to alginate, the mechanical properties of bioinks can be regulated to match the specific requirements of various tissues and organs.

NPs can also play an active role in both labeling and spatial organization. MNPs bound to the cell membrane or internalized within cells enable precise spatial organization of cellular assemblies under external magnetic field guidance, facilitating the formation of geometrically controlled organoids with high structural consistency. Through MNP adhesion to dissociated spinal cord cells, Bowser *et al.* successfully endowed the cells with magnetic properties and enabled highly reproducible assembly of spinal cord spheres.[80] Similar methods have also been successfully adapted for the cultivation of both salivary adenoid epithelial organoids and adipose tissue organoids.[81] The use of MNPs establishes a standardized platform for spheroid and organoid formation, ensuring the consistency in size and shape across batches. This technology reduces operator dependency, while significantly improving the reproducibility of 3D biostructure cultivation process.

2.3.2 Microreactors for organoid cultivation

2.3.2.1 Liquid marbles. Liquid marbles represent a novel class of biological microreactors characterized by a liquid culture core enveloped within a hydrophobic nanoparticle shell, exhibiting typical diameters in the millimeter scale (Fig. 3a). In these bioreactors, nanomaterials serve dual functions: (1) as semi-permeable encapsulation barriers that maintain system isolation, and (2) as gas–exchange interfaces between the liquid core and the external environment. Aalders *et al.* engineered cardiac organoids by encapsulating a cardiomyocyte-fibroblast suspension within hydrophobic fumed silica nanoparticles.[82] Brevini *et al.* demonstrated that hydrophobic polytetrafluoroethylene (PTFE) nanoparticles could encapsulate cellular suspensions, facilitating the formation of 3D aggregated cell spheres.[41] While liquid marble technology promotes cell aggregation and scalability needs, critical gaps remain in manual operation requirements and limited control over the microenvironment.

2.3.2.2 Nano-microwell culture system. Compared to liquid marble techniques, the microwell chip culture system provides superior control cell distribution in organoid culture and enable high-throughput production. Typically composed of polymer membranes with micropores, the microwell chip culture system incorporates surface-patterned hydrogels (*e.g.*, agarose and meth acryloyl gelatin (GelMA)) fabricated *via* 3D printing. The uniform-sized pores not only provide a supportive matrix required for cell growth but also constrain pore geometry to promote cell self-assembly and functional tissue formation.[84,85] It has been demonstrated to enhance the spheroid formation and enable precise gradient size control.[86] The platform facilitates high-throughput organoid cultivation under standardized conditions, thereby significantly improving experimental efficiency and reproducibility. This platform holds substantial promise for preclinical applications and scalable manufacturing, emerging as the predominant methodology for spheroid culture.[87] However, reliance on non-physiological polymer substrates may compromise organoid development. Impermeable microporous materials such as

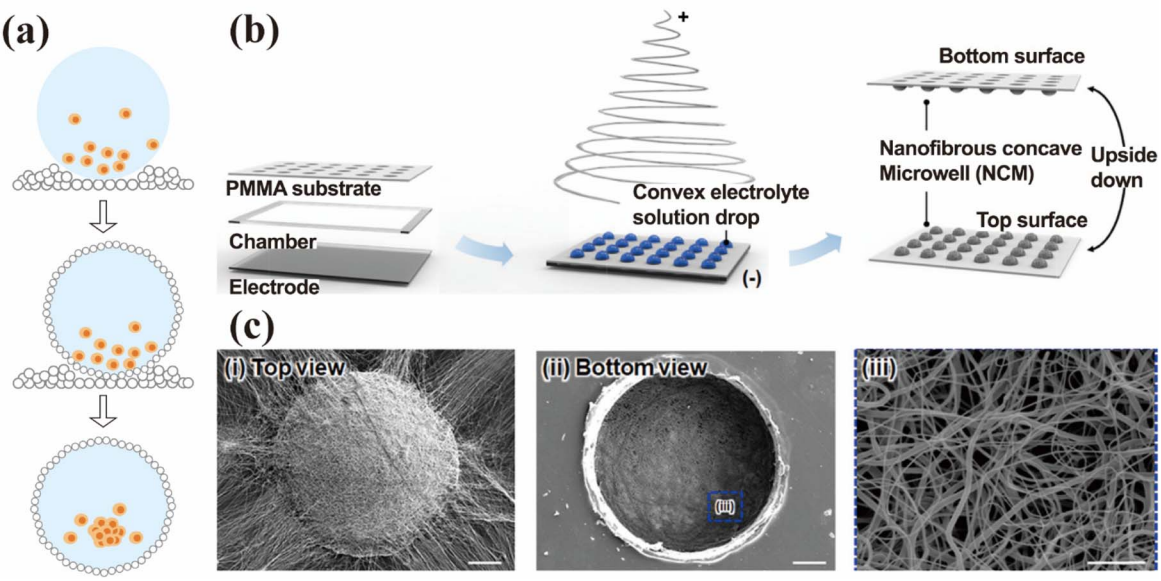

Fig. 3 Microreactor for organoid cultivation. (a) Schematic of liquid marble preparation and organoid cultivation. Cell suspensions were placed on the surface of hydrophobic nanoparticles and encapsulated *via* droplet rolling. The hydrophobic shell enables gas exchange between the droplets and the external environment while promoting cell aggregation and spheroid formation. (b) Schematic of the hydrogel-based U-shaped microwell array fabrication. U-shaped microcavities were fabricated on silicon substrates using a combination of Bosch processes and soft lithography. A PDMS mound was fabricated by replica molding the silicon substrate. The microcavities were then transferred to the hydrogel surface during cross-linking. (c) SEM images of nanofibrous microwells fabricated *via* electrospinning using both an electrolyte solution and a metal collector. This figure has been adapted/reproduced from ref. 83 with permission from the American Chemical Society, copyright 2018.

PDMS exhibit constrained mass transport properties, significantly limiting their application in organoid culture systems.

In 2016, Shin *et al.* developed a serum-free, xeno-free microporous 3D culture system utilizing a nanofiber-hydrogel composite for human salivary gland globule organoid cultivation.[88,89] The microporous culture system comprises a PCL nanofiber substrate integrated with PEG hydrogel micropore walls. The nanofibers fabricated by electrospinning form a highly porous network, effectively overcoming the mass transport limitations inherent to conventional polymer microporous systems. They can also influence the behavioral response of 3D cells and play a key role in regulating the spheroid size.[90] Surface modification of the fiber can enhance the cell adhesion behavior. Subsequent studies expanded on these findings to optimize the microporous reactor design. By employing convex hemispherical electrolyte droplets as a grounded collector for electrospinning, Park *et al.* developed a method to fabricate nanofiber-based concave micropores (NCM) with tunable shape and size (Fig. 3b and c).[83] Uniform and size-controlled human hepatocellular carcinoma cell line (HepG2) spheroids were successfully formed within the NCMs, exhibiting significantly enhanced metabolic activity compared to those cultured in 2D micropores. Kim *et al.* introduced a nanofiber-based elliptical microporous array, termed the NOVA microporous array.[91] The array exhibits an oval geometry with a wide opening, narrow bottom, high aspect ratio (AR) and high pore density. This design not only enhances cell capture efficiency within the micropores but also enables uniform and stable production of numerous viable and functional spheroids.

3. Nanomaterials for the cryopreservation of organoids

Organoids demonstrate significant application potential in fields such as disease modeling and drug screening. However, their clinical translation and large-scale adoption are constrained by challenges in long-term cultivation and storage, specifically during long-term culture and preservation. In particular, during extended expansion, organoids are prone to phenotypic drift and central necrosis.[92] Their complex 3D architecture and heterogeneous cellular composition render them highly sensitive to cryopreservation conditions, resulting in issues such as localized supercooling and insufficient cryoprotection. In conventional cryopreservation protocols, the widely used CPA dimethyl sulfoxide (DMSO) exhibits cytotoxicity.[93] Moreover, due to their size, organoids require extended periods for CPA permeation, thereby increasing their exposure to toxic damage.[94] Second, conventional water bath rewarming exhibits a lower heat transfer efficiency than the required critical warming rate (CWR).[95] Ice recrystallization induced by the temperature gradients during warming inflicts severe mechanical damage on cells. Consequently, the development of advanced cryopreservation and rewarming technologies has become a critical priority in the field of organoid research and application.

Nanomaterials present a novel strategy to overcome the challenges described above. In contrast to traditional CPAs, nanomaterials can act as auxiliary nucleation sites to regulate ice crystal formation and reduce the risk of supercooling.[96]

Nanomaterials can also modulate ice crystal growth kinetics and enable the targeted delivery of CPAs such as trehalose, thereby enhancing cryopreservation efficiency. These advantages have allowed nanomaterials to demonstrate promising performance in the cryopreservation of various cell types.[97] Furthermore, certain functionalized nanomaterials can enhance cryopreservation outcomes through antioxidant effects and cell stabilization. Additionally, nanomaterials can serve as heating mediators during rewarming, promoting uniform and rapid temperature increase.[13] Therefore, elucidating the mechanisms of nanomaterials in organoid cryopreservation and exploring effective application strategies will provide crucial technical support for their long-term stable preservation and promote broader clinical and research application.

3.1 Current advances and challenges in organoid cryopreservation

Cryopreservation represents a core technology driving the large-scale application of organoids. To date, researchers have developed a variety of CPA formulations and corresponding cryopreservation protocols tailored for different functional types of organoids.[98] However, the inherent heterogeneity and complex cellular composition of organoids significantly impede the effectiveness of conventional CPAs and uniform heat transfer, presenting major challenges during both the freezing and thawing process.

3.1.1 Essential role of organoid cryopreservation in advancing biomedical research. Organoids, highly physiologically relevant 3D cell culture systems, not only recapitulate the complex architecture and physiological functions of specific human organs but also reproduce disease-specific pathological features, thereby offering an unprecedented platform for biomedical research.[99] For instance, using human intestinal organoids, Saxena *et al.* demonstrated that differentiated intestinal cells are more susceptible to human rotavirus (HRV) infection than undifferentiated cells.[100] Human cortical organoid models have demonstrated the metastatic potential of glioblastoma to select non-malignant organs.[101] Furthermore, genetic engineering of organoids enables the exploration of disease causation and pathological characteristics associated with gene mutations, representing an important advancement for disease modeling studies.[102,103]

From the application perspective, organoids advance drug development and personalized medicine, offering valuable alternative 2D cell cultures and animal models in high-throughput drug screening.[104–106] Studies employing endometrial and breast cancer organoids have enabled rapid screening of drug combinations and identification of effective tumor inhibitors, accelerating novel drug development.[107] Moreover, patient-derived organoids preserve genetic traits and reduce disease heterogeneity, providing a platform for developing personalized treatment plans.[108,109] For instance, studies utilizing organoid models have successfully identified effective drugs for aggressive diseases such as triple-negative breast cancer.[2] Moreover, organoids could function as a bridge therapy to stabilize patients awaiting organ transplantation, exhibiting significant potential in the field of transplant medicine. Compared with allogeneic organ transplantation, organoids derived from autologous stem cells present significantly lower risks of immune rejection. Current research has successfully demonstrated the transplantation of the liver, pancreas, intestine, and other organoid types in mouse models, showing evidence of therapeutic efficacy in disease treatment.[110] Nevertheless, the functional mechanism and immunogenic potential of organoids remain incompletely characterized.

Despite the demonstrated potential of organoid technology in both fundamental research and clinical applications, challenges in long-term stable preservation remain a critical limitation for its widespread application.[111] Organoids may undergo phenotypic drift and genetic instability due to prolonged *in vitro* culture conditions and serial passaging, potentially compromising their clinical application. Since many diseases demonstrate progressive pathophysiology, organoid phenotypic instability distorts disease progression studies and causes time-dependent model variations, severely restricting their utility for mechanism exploration. Similarly, phenotypic discrepancies between organoids and native tissues may compromise drug screening accuracy and personalized medicine, leading to unreliable therapeutic predictions.[92] The cryopreservation of organoids during early developmental stages minimizes the passage-induced phenotypic drift, improving model consistency.[98] Batch-cryopreserved organoids enable reproducible experimentation by allowing repeated utilization of genetically matched models across multiple timepoints, ensuring experimental consistency.

Cryopreservation technology holds a critical value for both organ transplantation and biobanking, enabling long-term storage of viable biological specimens.[112] Current culture conditions enable short-term maintenance of organoids, and room temperature storage/transport preserves their active function.[113,114] However, the absence of long-term preservation methods leads to loss of cell viability, impaired structural integrity and functional decline of organoids. These limitations significantly compromise organoids' reliability as an experimental model while hindering their translational potential, particularly for multi-institutional studies and large-scale clinical applications. Cryopreservation significantly reduces the cellular metabolic rate and enables on-demand availability of viable biological products for therapeutic use. Cryopreservation is essential for maintaining the viability and functionality of organoids during storage and transport, ensuring their availability for experimental, therapeutic, and clinical applications.

3.1.2 Size- and heterogeneity-dependent challenges in organoid cryopreservation. The standard cryopreservation comprises four critical phases: co-incubation with CPAs, cooling stage, long-term storage, and thawing. The cryopreservation of suspended cells operates on a microscale, where short mass/heat transfer distance (cellular radius) ensures the uniform diffusion kinetics for water, solutes, and thermal energy between cells and their environment.[115] However, when cryopreservation is scaled up to 3D spherical structures and organoids, the low efficiency of mass transfer and heat transfer

significantly increases the complexity of cryopreservation process.

During CPA incubation, organoids exhibited volume changes similar to suspended cells: initial dehydration and shrinkage due to the water efflux, followed by gradual volume recovery as the CPA permeated the cells.[116] The key difference is that, due to their large size, outer cells experience a prolonged osmotic equilibration period, making them more susceptible to osmotic damage and cytotoxic effects.[94] The cell osmotic pressure in the central region is maintained at a low level, which may impair CPA diffusion. In addition, the mass transfer process involves both intracellular transport and ECM diffusion. The overall process is challenging to control, resulting in inconsistent cryoprotection efficacy that ultimately compromises the 3D structural integrity.[117,118] While increasing the CPA concentration and incubation temperature may effectively address these challenges, careful optimization will be required to balance efficacy with potential cytotoxicity. CPA diffusion is driven by the concentration gradient; therefore, increasing the external CPA enhances the driving force, leading to faster CPA penetration rates and shorter incubation times.[119] However, this approach must be carefully balanced, as high CPA concentration exhibits significantly greater cytotoxic effects. In addition, the temperature critically influences CPA penetration efficiency, while a lower temperature reduces the intracellular enzyme activity. At room temperature, elevated cellular metabolic activity promotes more efficient material exchange, enabling significant reduction of CPA incubation time.[120] However, the CPA cytotoxicity accelerates at room temperature compared to lower temperatures.[121,122] Therefore, appropriate CPA concentration, incubation temperature and exposure duration are all crucial for effective cryopreservation.

During the initial stage of cooling, CPA loading is completed, and mass transfer processes, including cellular metabolism, can be neglected. The rapid heat exchange between the outer surface of organoids and the surrounding environment makes the initial cooling rate a critical factor in minimizing cellular damage. Ultra-slow cooling rates may induce mechanical damage due to the excessive ice crystal growth.[123] During the ultra-rapid cooling, the osmotic imbalance across the plasma membrane drives excessive water efflux, resulting in cell shrinkage and damage. This may also induce solution supercooling, followed by explosive crystallization at a critical temperature. The subsequent rapid release of latent heat generates substantial internal mechanical stress, potentially causing structural damage.[116] During ice formation, the propagating mechanical stress is transmitted through intercellular connections, resulting in the disruption of the 3D architecture of organoids.[124,125] Similarly, during rewarming, precise control of thermal gradient is essential for ensuring uniform heating. Notably, the 3D heterogeneous architecture of organoids significantly influences heat conduction rates and temperature distribution. The low inconsistent heat conduction rate within organoids leads to a substantial internal temperature gradient, prolonging the thermal equilibration time and exacerbating the risk of thermal stress-induced damage.[126] Therefore, optimizing heat transfer uniformity and temperature distribution homogeneity represents the critical breakthrough needed to resolve dynamic temperature control challenges in organoid cryopreservation.

Furthermore, cellular and dimensional heterogeneity presents a fundamental challenge in organoid cryopreservation. In large-sized organoids, restricted internal mass transfer limits uniform CPA diffusion, significantly increasing the risk of lethal intracellular ice formation during cryopreservation. Small or immature organoids are more sensitive to osmotic stress owing to their elevated metabolic rates, increasing susceptibility to membrane rupture or apoptosis. The cryopreservation requirements of organoids vary significantly across developmental stages, tissue types and physical dimensions, while inherent cellular heterogeneity further complicates protocol optimization.[127] Organoids typically comprise heterogeneous cell populations at varying developmental stages with distinct physiological functions. This cellular diversity manifests in differential cell membrane composition, variable CPA permeability coefficients, and dehydration kinetics during cryopreservation.[128] For example, the membrane permeability to ethylene glycol (EG) in granulocytes is much higher than that of DMSO and glycerol. Similarly, the permeability of stem cells to glycerol and DMSO is also different.[129] The standard intestinal organoid model comprises multiple cellular components including stem cells, epithelial cells, goblet cells, and endocrine cells, each exhibiting distinct cryosentivity.[130] During cryopreservation, heterogeneous cell populations within organoids exhibit differential responses to identical freezing conditions. Developing precision cryopreservation protocols that account for this cellular diversity represents a critical challenge requiring innovative solutions.

3.1.3 Limitations of traditional cryoprotectants in organoid preservation. Current organoid cryopreservation strategies primarily employ two approaches: slow freezing and vitrification. Slow freezing is the most common method for organoid cryopreservation, typically employing a combination of 10% DMSO and 90% fetal bovine serum (FBS) as CPAs. Following combination with CPAs, organoids are incubated for 0.5–2 hours under the culture conditions to facilitate CPA penetration into the core. A controlled cooling rate of -1 °C min^{-1} is then applied to -80 °C, after which the samples are transferred for long-term storage at -150 °C or liquid nitrogen (-196 °C).[131–133] Vitrification preservation requires stepwise exposure to increasing concentrations of CPAs to mitigate osmotic stress. For vitrification, organoids are first equilibrated in a low-concentration protective solution (*e.g.*, 10% DMSO) for 1–10 min. They are then transferred to high-concentration vitrification solution, typically containing 20% DMSO, EG, and other CPAs, for a brief incubation (~30 s). Immediately following this short exposure, the organoids are directly plunged into liquid nitrogen for cryopreservation.[134,135] Compared to traditional slow freezing, vitrification demonstrates superior outcomes for a wide range of cells and tissues, significantly enhancing the post-thaw viability and proliferation rates.[134] To enhance cryoprotectant permeation and reduce thermal mass, organoids were dissociated into smaller clusters or single cells prior to CPA loading. A significant drawback of

this approach is the destruction of the original 3D structure, necessitating a cumbersome post-thaw recovery culture to restore it. This entire process can adversely affect the morphology and function of organoids.[113,136]

Although DMSO is an effective cryoprotectant, its inherent cytotoxicity can damage the cell structure and function. Furthermore, DMSO can induce the denaturation of proteins and other biological molecules, adversely affecting the functionality of cells upon thawing.[137] Consequently, researchers worldwide have conducted extensive studies aimed at reducing the required concentration of DMSO and identifying less cytotoxic alternative CPAs.[138] For example, studies on various cell types have demonstrated that a combined CPA solution containing a lowered concentration of 5% DMSO significantly improves post-thaw cell survival and function compared to higher concentrations.[139] However, a DMSO concentration exceeding 15% drastically reduces survival due to extreme osmotic damage and cytotoxicity. Consequently, the development of novel, less toxic CPAs and advanced cryopreservation techniques has become a critical research frontier, essential for enabling the broader applications of organoid technology.

3.2 Cryopreservation mechanism and application of nanomaterials

Nanomaterials have demonstrated a remarkable capability to regulate ice crystal formation and growth, thereby preventing ice crystallization-related damage during cryopreservation. Furthermore, they facilitate the intracellular delivery of non-permeable CPAs such as trehalose (Fig. 4). Recently, research into and application of nanomaterials for cryopreservation have expanded significantly, establishing them as promising emerging strategies to overcome the challenges of conventional cryopreservation protocol.[13]

3.2.1 Nanomaterial-based cryoprotective mechanisms. As previously stated, the osmotic, mechanical and thermal stress damage resulting from ice nucleation and growth primarily contributes to cell death after cryopreservation. Thus, the effective regulation of ice crystal formation and growth is essential for enhancing the cryopreservation outcome.

The presence or absence of impurities distinguishes the two primary mechanisms of ice nucleation: homogeneous nucleation and heterogeneous. During cooling, the CPA solution lowers the freezing point but often lacks sufficient nucleation sites, leading to significant supercooling. While some studies have attempted to induce ice nucleation manually, this approach suffers from poor reproducibility and risk of localized rapid crystallization, which cause damage to cells.[140,141] To address this, nanomaterials can serve as heterogeneous nucleating agents by providing a high density of nucleation sites, which promotes uniform ice nucleation and reduces supercooling. The ice nucleating ability of carbon-based nanomaterials was first demonstrated by Whale *et al.*[142] Subsequent investigation studies have revealed that nanomaterials such as nanocrystalline cellulose, MoS_2, and silica can act as effective nucleation sites to control ice nucleation, a process influenced by their morphology and size.[143,144] The ability to promote ice nucleation is generally stronger in smaller nanoparticles, while larger nanoparticles often exhibit an inhibitory effect. However, the influence of nanoparticle morphology on ice nucleation remains poorly understood and lacks consensus. In addition to promoting ice nucleation, nanomaterials offer additional benefits of limiting ice growth, regulating crystal morphology, and inhibiting recrystallization. Research has shown that nanomaterials with special functional groups and molecular structures such as GO, quasi-carbon nitride quantum dots, and metal–organic framework (MOF) nanoparticles can bind to the

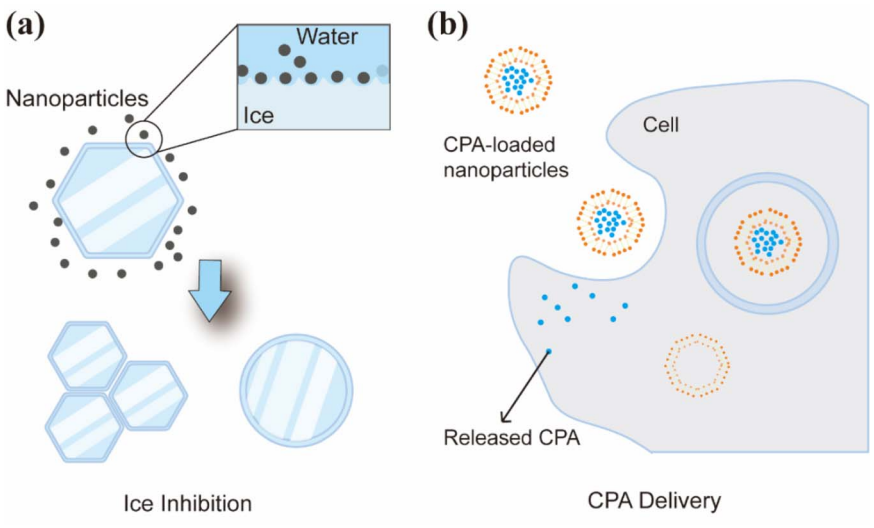

Fig. 4 Cryoprotective mechanism of nanomaterials in cell cryopreservation primarily operates *via* two key pathways. (a) Ice crystal regulation. Nanoparticles (NPs) interact directly with water molecules to inhibit the uncontrolled growth of ice crystals. This interaction modulates ice crystal morphology, promoting the formation of smaller, more uniform crystals, thereby reducing the mechanical damage to the cellular structure. (b) Delivery of non-permeable cryoprotectants (CPAs). NPs function as carriers for non-permeable CPAs such as trehalose. They facilitate the intracellular delivery of these compounds, thereby achieving superior protective effects.

Table 2 Applications of nanomaterials in cryopreservation[a]

Nanomaterials		Cells	Function	References
Apatite nanoparticles		Sheep RBCs	Trehalose delivery	147
pH-responsive genipin-cross-linked pluronic F127-chitosan nanoparticles		Primary human adipose-derived stem cells		148
Cold-responsive trehalose-laden nanoparticles		MDA-MB-231 cancer cells and human ASCs		149
Chitosan-TPP nanoparticles		Natural killer-92 cells		150
Nanohydrogel (acrylamide-type polymer network)		Human umbilical vein endothelial cells		151
Carbon derivatives	GO		Inhibition of ice crystal growth	96
	Fe_3O_4 deposited GO	Human MSCs		152
	OCNQDs and S-OCNQDs	Sheep RBCs		153
	Graphene nanoparticles	—		154
	G-CDs	Sheep RBCs		155
Metal nanomaterials	Iron oxide	Mice oocytes	Inhibition of ice crystal growth, uniform rewarming	156
	Ti_3C_2	Human MSCs		157
	MoS_2	Human lung cancer cells (A549 cells)		144
Organic-inorganic metal materials	Nano-zirconium-based MOF	Human RBCs	Inhibition of ice crystal growth	158
	Two-dimensional MOLs of Hf	Human RBCs		145
	PEG-gold hybrid nanoparticles	—		159
	Gold nanoparticles grafted with peptide nanofibrils	—		160
	Fe_3O_4@SiO_2 nanorods	Porcine artery models	Inhibition of ice crystal growth, uniform rewarming	161
	Combination of carbon dots and gold nanorods by SiO_2	Hela cells		146
Polymer nanomaterials	$PGMA_{56}$-$PHPMA_{155}$/PVA system	Ovine RBCs	Inhibition of ice crystal growth	162
	PVA_{181}-g7-$PHPMA_n$	—		163
Nanomotor with magnesium/palladium covering one side of a silica platform (Mg@Pd@SiO_2)		Normal colon epithelial (NCM460) cell *Ex vivo* tissues (small intestine, liver, and kidney)	Inhibition of ice crystal growth, reducing oxidative stress, uniform temperature profile	164

[a] RBCs: Red blood cells; ASCs: Adipose tissue-derived stem cells; TPP: Tripolyphosphate; GO: Graphene oxide; MSCs: Mesenchymal stem cells; OCNQDs: Oxidized carbon nitride quantum dots; S-OCNQDs: Sulfur-doped carbon nitride quantum dots; G-CDs: Glucose-derived carbon dots; MOF: Metal organic framework; MOLs: Metal–organic layers; Hf: Hafnium; PEG: Poly(ethylene glycol); PGMA: Poly(glycidyl methacrylate); PVA: Poly(vinyl alcohol); PHPMA: Poly(hydroxypropyl methacrylate).

basal or prismatic planes of ice crystals. This binding inhibits ice growth and regulates the morphology of crystals (Table 2).[145,146]

The high thermal conductivity of common nanoparticle constituents including metals, metal oxides, and carbon-based materials enhances thermal management during cryopreservation. The incorporation of high-thermal-conductivity nanoparticles into CPAs facilitates the formation of effective heat conduction pathways. These pathways accelerate the thermal transport, which consequently enhance the overall thermal conductivity of the solution.[165] In addition, the Brownian motion of nanoparticles makes them more evenly distributed in the solution. This homogeneity helps to eliminate local hot spots, thereby promoting uniform temperature changes throughout the freezing phase.[161] The uniform cooling process mitigates the irregular formation of ice crystals and alleviates the possibility of cell damage due to ice crystals.

The generation of reactive oxygen species (ROS) during freezing and thawing processes presents a major threat to cell survival. Therefore, antioxidants such as glutathione are commonly incorporated into commercial organoid cryopreservation reagents to mitigate ROS-induced damage. However, these protective agents themselves can adversely affect essential cellular functions.[166,167] Due to their large specific surface area and abundant surface-active sites, nanomaterials can effectively capture free radicals during the freeze-thaw process, thereby preventing oxidative harm.[168–170] In addition, these sites can bind to biological macromolecules, such as proteins on the cell membrane, to form a protective layer on the cell surface. This layer provides an additional physical barrier that improves membrane stability, thereby mitigating rapid water loss and exposure to high concentrations of protective agents. This effect reduces osmotic pressure damage;[33,171] however, the dosage must be carefully controlled to avoid potential damage to the antioxidant system by excessive nanoparticles.[172]

Beyond their intrinsic benefits, nanomaterials can act as carriers to deliver non-permeable protective agents such as trehalose into cells, thereby maximizing protection. Trehalose

is a natural and widely used non-permeable CPA found in many organisms. However, as mammalian cells cannot synthesize it, trehalose can only provide optimal cryoprotection when present on both sides of the membrane.[173] To facilitate intracellular delivery of trehalose, various techniques have been employed, including electroporation, thermal shock, and microinjection.[174–176] However, these strategies cause damage to the cell membrane to varying degrees. Furthermore, their strict technical requirements hinder their use in mass cell treatment. Endocytosis-driven nanovector delivery offers a more biocompatible platform for trehalose transport, bypassing the need for additional clearance mechanisms.[177]

3.2.2 Nanomaterials for mediating cell and tissue cryopreservation. The delivery of nanomaterials within CPAs enhances cellular and tissue cryopreservation outcomes. In 2009, Zhang *et al.* developed the first thermally responsive polymer hydrogel-based nanocapsule for the encapsulation and intracellular delivery of trehalose.[178] Following a 40 minutes incubation period, fibroblasts achieved an intracellular trehalose concentration of up to 0.3 M, which consequently led to a significant improvement in cryopreservation. In subsequent studies, the incorporation of targeting ligands enabled the nanomaterials to bind specific receptors, significantly enhancing cellular recognition and uptake of the nanocapsules. Furthermore, these nanomaterials were designed to be stimuli-responsive, allowing for targeted and controlled drug release.[151]

Another major application focuses on controlling ice crystallization and stabilizing outer cell membranes. For instance, Xu *et al.* studied how ice-suppressing micro–nano materials of different sizes affect the cryopreservation of various cell types, such as human umbilical vein endothelial cells, mouse myoblasts, and bovine mammary epithelial cells. The study revealed that a smaller particle size enhanced the cryoprotective efficacy of the carbon complex particles.[179] Compared to spherical particles, asymmetric and flower-like nanomaterials significantly improved cell cryopreservation outcomes. Owing to their good biocompatibility and modifiable surface properties, these nanomaterials can adapt to various conditions and provide new solutions for spheroid and organoid cryopreservation. Gao *et al.* reported the use of a magnesium/palladium-covered silica nanomotor (Mg@Pd @SiO_2) for highly efficient cryopreservation.[97] The nanomotor alleviated freezing damage in cells and tissues by inhibiting ice crystallization. The mechanism involves the release of Mg^{2+} ions and hydrogen gas (H_2) upon cooling in solutions. The subsequently promoted adsorption of H_2 at the palladium binding site on the cell surface effectively suppresses ice crystal formation. During the thawing process, the nanomotor switched from a dormant state to an active one upon laser activation, enabling the continued release of H_2. This approach further restrained ice recrystallization and minimized cell and tissue damage. The team demonstrated that these nanomotor significantly improved both the survival rate and the functional recovery of NCM460 cells. The technology also proved effective in protecting isolated tissues from the small intestine, liver and kidney tissues, demonstrating its potential for organoid cryopreservation.

Despite the multiple advantages that nanomaterials offer for enhancing cell cryopreservation, particular attention must be paid to their permeability when utilized with 3D models such as spheres and organoids. The complex 3D architecture and high cell density of organoids hinder the uniform penetration of CPAs and nanomaterials, currently limiting their application in cryopreservation. In a study, supplementing traditional CPAs with non-permeable chemical nucleating agents effectively improved the survival rate of spheroids after thawing, indicating the significant potential of nucleating agents in cryopreservation.[180] Further research has found that anionic nanoparticles can open the tight junctions between intestinal epithelial cells, thereby acting as penetration enhancers for physical and chemical drugs.[181] Since this effect is reversible and non-damaging, it presents a new promising approach for enhancing CPA diffusion in intestinal organoids.

3.3 Nanomaterials for organoids thawing

The rewarming of suspended cells is typically performed in a 37 °C water bath. Agitating the cell suspension during thawing promotes efficient heat conduction, shortens the time window for ice crystal formation, and prevents recrystallization. However, for large cell spheroids and organoids, the heat transfer efficiency of water bath rewarming decreases significantly, resulting in a heating rate that falls below the CWR necessary for cells and organ survival. The substantial temperature gradient between the surface and the center promotes ice recrystallization, which causes fatal mechanical damage to the cells within the organoid.[182,183] Nevertheless, the conventional approach of thawing in a 37 °C water bath for 2–3 min remains the most commonly used thawing method for globules and organoids. This protocol is a standard practice following both slow freezing and vitrification.[132,141,184,185] Although dissociation or sectioning organoids prior to thawing reduces cell damage, it increases subsequent culture time and cost. Therefore, there is an urgent need to develop new rewarming protocols that can achieve a higher CWR for intact organoids.

Microwave radio frequency heating rapidly thaws cells, tissues, and organs by exciting water molecules to absorb energy and convert it into heat.[182,186] However, the uniformity of heat transfer is often compromised by CPA composition, which may result in local overheating and increased thermal stress damage.[183] The limited penetration depth of microwave radiation also prevents uniform rewarming, particularly in large-sized samples, where it creates significant thermal gradients. Advances in nanotechnology have enabled the use of nanoparticles as highly efficient heating media for biomaterials, including laser nano-heating and radio frequency (RF) nano-heating.

3.3.1 Laser nano-heating. Laser pulse heating enables rapid local heating, making it particularly suitable for applications requiring precise control over the heating area and rate. In this approach, nanoparticles are commonly employed as photothermal conversion agents. They absorb laser energy and convert it into heat energy, thereby facilitating rapid sample heating (Fig. 5a). The photothermal properties of non-carbon

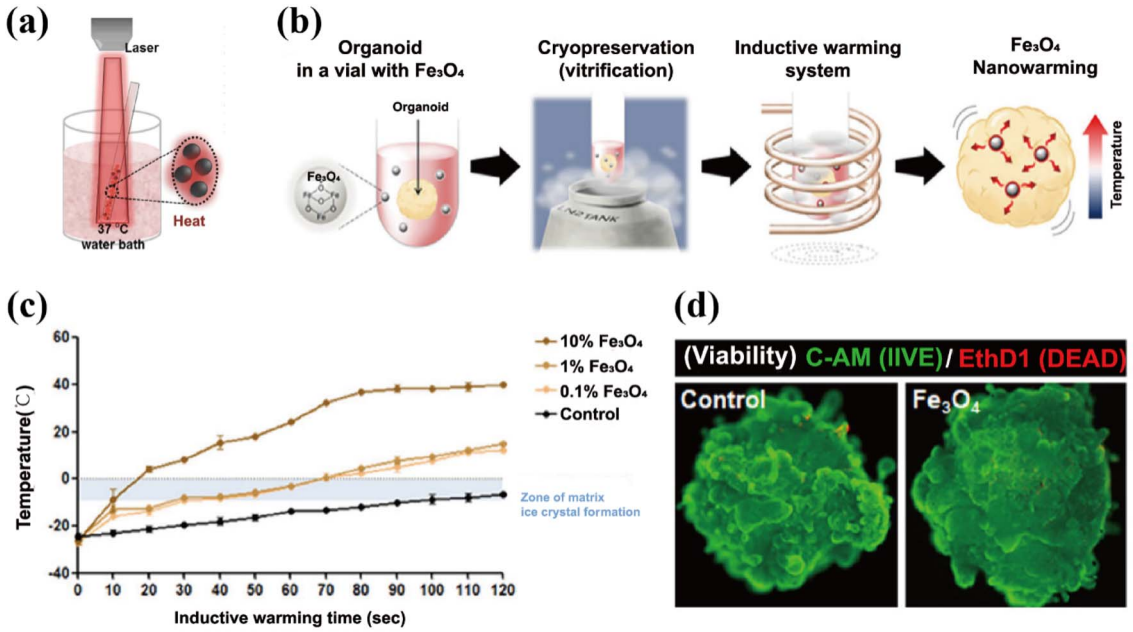

Fig. 5 Nano-thawing for organoid cryopreservation. (a) Schematic of laser-nano heating. Cryopreserved samples were placed in a 37 °C warming solution and subjected to a near-infrared laser field at an intensity of 1000 mW cm^{-2} for 10 s to induce photothermal effects, followed by additional 5 s of rewarming. This figure has been adapted/reproduced from ref. 188 with permission from Elsevier Ltd, copyright 2019. (b) Schematic of radio frequency (RF)-based nanoheating. Organoids were loaded onto vials containing cryoprotectants (CPAs) and Fe_3O_4 nanoparticles, vitrified in liquid nitrogen, subsequently rewarmed *via* RF excitation of the Fe_3O_4 particles surrounding the organoids. (c) Temperature profiles of samples with different concentrations of Fe_3O_4 (0.1%, 1%, and 10%) measured over the warming period. Data are presented as mean ± SD. $n = 3$. (d) Viability comparison between 0% and 10% Fe_3O_4 groups assessed using the LIVE/DEAD assay. $n = 5$. This figure has been adapted/reproduced from ref. 13 with permission from John Wiley & Sons, Inc., copyright 2023.

nanomaterials such as carbon black, GO, gold nanoparticles, and molybdenum disulfide have been extensively studied. These agents have been successfully applied for the rewarming of small-sized biological samples such as oocytes.[187] Compared to traditional water bath rewarming, laser pulse heating provides more precise energy input and makes the heating process more controllable. Unfortunately, its poor penetration depth prevents its application for larger and more complex samples like organoids.[188] Recently, soft Pluronic F127-liquid metal nanoparticles (PLM NPs) have been used as highly efficient photothermal conversion agents. These nanoparticles demonstrate superior efficiency in converting light energy into heat energy, and have yielded improved outcomes for the thawing of mouse tail tissues.[189] Alvarez *et al.* developed a beam splitting laser system that uses TiN as a photothermal conversion agent to uniformly heat cryopreserved biological samples at multiple angles with beams of the same energy, significantly enhancing the heating rate and range, which opens up a new possibility for the vitrification of cell spheres and organoids.[190]

3.3.2 Radio frequency (RF) nano-heating. Radio frequency (RF) nano-heating utilizes MNPs such as iron oxide. Under an external magnetic field, MNPs generate heat through a magnetic relaxation loss mechanism. Furthermore, their position can be guided by an external magnetic field, enabling precise thermal targeting of specific areas (Fig. 5b).[191] In addition, the alternating magnetic field exhibits deep tissue penetration, capable of permeating the entire organ without decaying. The thawing process can be adapted to the needs of different organs by controlling the amplitude and frequency of the magnetic field, as well as the type and size of MNPs. An alternating magnetic field frequency of 300–800 kHz, combined with approximately 10 nm magnetite (Fe_3O_4) MNPs, is essential for achieving the ultra-high heating rate required to effectively inhibit ice recrystallization (Fig. 5c).[192]

As early as 13 years ago, Etheridge *et al.* demonstrated the use of magnetic nanoparticles to achieve faster and more uniform rewarming in kidney models.[193] Further studies revealed that magnetic heating not only reduced internal stress but also reversed its distribution, transferring stress capable of causing cracks toward the outer wall. The residual stress accumulated during the freezing process acts as a buffer, allowing for a higher heating rate by resisting the additional stress generated during rapid rewarming. This mechanism further demonstrates the application potential of magnetic heating in biological tissue thawing. Wakabayashi *et al.* systematically studied the effects of magnetic field frequency, magnetic nanoparticle concentration, and sample size on nano-rewarming.[194] The study revealed that the heating rate was promoted by increases in magnetite concentration, applied power, and field frequency, independent of the sample volume. A concentration of 5 mg mL^{-1} iron oxide nanoparticles achieved the CWR. However, considering the potential complications associated with higher concentrations, they identified the optimal rewarming condition as 5 mg mL^{-1} nanoparticles, 10

KW power, and 208 kHz frequency. Their research provides a theoretical basis for the application of MNP-mediated rewarming in organoid cryopreservation. Subsequently, Lee *et al.* successfully applied the previously reported iron oxide nanoparticles to rewarm heart-like organs exceeding 2 mm in diameter. This approach achieved a faster and more uniform heating profile than traditional water baths. This led to significantly improved morphological and functional recovery in the thawed organs (Fig. 5d).[13]

3.3.3 Limitations of nano-thawing technology. Although nano-rewarming effectively enhances the rewarming efficiency of organoids, several limitations still remain. A primary concern is the potential toxicity of nanomaterials. While some studies have employed strategies such as manganese ion doping and incorporation of other elementals to enhance the heating performance, minimizing the inherent toxicity of both the material cores and the dopant continues to be a critical challenge for future research.[195] In addition, the aggregation of nanoparticless poses another significant challenge. Commonly used CPA solutions typically consist of mixtures of organic solvents and inorganic salts with high ionic strength, which can induce the aggregation of unmodified nanoparticles.[196] This non-uniform distribution can result in local overheating within the organs, elevating the risk of thermal stress-induced damage.[197] Surface modification of nanoparticles such as coating represents a promising strategy to simultaneously overcome both issues. Surface modification can enhance the spatial repulsive forces among nanoparticles, thereby promoting their stable dispersion within CPA solution and reducing the tendency of aggregation. Furthermore, coating can effectively encapsulate the nanoparticles, mitigating the release of cytotoxic components. However, the introduction of a surface coating may impede heat generation and consequently reduce the rewarming rate. It is therefore necessary to strike a balance between achieving rapid rewarming and minimizing adverse effects, as well as to systematically identify appropriate coating materials.

Building upon iron oxide nanoparticles, Manuchehrabadi *et al.* developed a coated mesoporous silica structure that effectively prevented the precipitation of magnetic nanoparticles and greatly improved their biocompatibility.[198] The experimental results across various cell types and tissue models have further confirmed the superiority of magnetic nanoparticle-mediated heating during rewarming over traditional water bath convection methods. Similarly, PEG-coated superparamagnetic iron oxide nanoparticles synthesized by Chiu-Lam *et al.*,[191] PEG-modified silica-coated iron oxide nanoparticles reported by Karimi,[199] and nanoparticles described in other studies all exhibit comparable stability and satisfactory rewarming effects.[200] Joshi *et al.* investigated the mechanical stress induced by silica-coated iron oxide nanoparticles (SiONPs) during the rewarming of rat hearts and human heart models and found variations in the heating rates among different regions of the samples.[197] Areas that rewarm more rapidly experience compressive stress, whereas regions heating more slowly are subjected to tensile stress. Such non-uniform thermal stresses pose a greater threat to the structural integrity of vitrified samples. Furthermore, the study indicated that the location and magnitude of the maximum stress during the rewarming vary with the concentration of SiONPs, though no consistent pattern has yet been established. In addition, Liu *et al.* suggested that encapsulating stem cells within hydrogels embedded with magnetic nanoparticles can prevent direct physical contact between the cells and the nanoparticles. This strategy not only ensures the heating efficiency but also eliminates potential cytotoxicity, showing promising applicability for the rewarming of organoids.[201]

Hypothermic perfusion also serves as a method to promote the uniform distribution of nanoparticles throughout different regions of biological tissues.[202] In contrast to direct incubation, this approach enables homogeneous nanoparticle distribution throughout the organ, enabling heat generation to initiate from within the organoids and diffuse outward. This method facilitates accelerated heating rates and enhanced thermal uniformity, making it particularly suitable for the cryopreservation of large tissues and organs. However, its application depends on the presence of a fully developed vascular system, which limits its use in most organoid models.

4. Summary and future prospects

This review explores the current applications of nanomaterials in organoid culture and cryopreservation and discusses the major challenges associated with the freezing and recovery of organoids. As 3D *in vitro* models, organoids show great potential for applications in drug screening, disease modelling and other biomedical fields, with the additional advantage of avoiding ethical controversies. However, their broader adoption remains hindered by challenges such as poor reproducibility, difficulties in synchronizing heterogeneous cellular developmental stages, and the limitations of current cryopreservation techniques. Nanomaterials have demonstrated revolutionary potential in both organoid construction and cryopreservation owing to their distinctive physicochemical properties. In organoid fabrication, functionalized nanomaterials can modulate the properties of hydrogel matrices to allow dynamic control over structural stiffness. Furthermore, nanomaterials can guide cells to assemble into specific geometric configuration, thereby facilitating the reproducibility of organoid cultures. In the context of cryopreservation, nanomaterials exhibit considerable application potential by effectively suppressing ice crystal formation, achieving targeted delivery of CPAs and enabling uniform rewarming.

Nonetheless, current research still confronts several challenges. First, our understanding of cellular behavior remains inadequate to precisely define the nutritional demands and matrix microenvironment required at various developmental stages. Moreover, the specific impacts of nanomaterial-modified matrix gels on cellular functions and phenotypes have not yet been fully elucidated. Second, the long-term safety of nanomaterials raises another critical concern. Finally, the inherent heterogeneity of organoids means that cryopreservation outcomes are highly dependent on the type and concentration of the nanomaterials used, with results varying not only

between organoid types but also within replicates of the same type. The development of precise, tailored cryopreservation methods to address the heterogeneity of organoids constitutes a pivotal challenge that must be urgently addressed.

The application of artificial intelligence (AI) in organoid construction and cryopreservation represents a cutting-edge frontier in biomedical research. Leveraging machine learning (ML) to predict nanomaterial–organoid interactions enables the rational design of materials aimed at reproducible culture and personalized cryopreservation protocols. In addition, the ML models can be trained on data from previous experiments to predict the cytotoxicity and efficiency of novel nanomaterial-based CPA combinations, optimizing for multiple objectives simultaneously, such as maximizing post-thaw viability, minimizing phenotypic drift, and maintaining functionality. AI can also model the complex heat and mass transfer processes during cryopreservation. Enhancing the integration of nanomaterials and biosensors to enable dynamic monitoring of organoid development and cryopreservation would provide deeper insights into the underlying cellular mechanisms. With multidisciplinary collaboration and continuous advancements in materials science and methodology, organoid research is poised to enable broad medical applications and drive significant innovation in healthcare.

Author contributions

Wanjuan He: Reviewing the literature and Writing – major part of the original draft. Qinlin Sun: Writing – part of the original draft. Dan Ge: Writing – review & editing. Bingbing Sun: Writing – review & editing and funding acquisition. Yang Liu: Conceptualization, supervision, writing – review & editing, and funding acquisition.

Conflicts of interest

There are no conflicts to declare.

Data availability

No primary research results, software or code has been included and no new data were generated or analysed as part of this review.

Acknowledgements

This work was supported by the National Key Research and Development Program of China (2022YFC2304305), the Fundamental Research Funds for the Central Universities (DUT20RC(3)035), and the National Natural Science Foundation of China (U22A20455).

References

1 Z. Zhao, X. Chen, A. M. Dowbaj, A. Sljukic, K. Bratlie, L. Lin, E. L. S. Fong, G. M. Balachander, Z. Chen, A. Soragni, M. Huch, Y. A. Zeng, Q. Wang and H. Yu, *Nat. Rev. Methods Primers*, 2022, **2**, 94.
2 K. P. Guillen, M. Fujita, A. J. Butterfield, S. D. Scherer, M. H. Bailey, Z. Chu, Y. S. DeRose, L. Zhao, E. Cortes-Sanchez, C. Yang, J. Toner, G. Wang, Y. Qiao, X. Huang, J. A. Greenland, J. M. Vahrenkamp, D. H. Lum, R. E. Factor, E. W. Nelson, C. B. Matsen, J. M. Poretta, R. Rosenthal, A. C. Beck, S. S. Buys, C. Vaklavas, J. H. Ward, R. L. Jensen, K. B. Jones, Z. Li, S. Oesterreich, L. E. Dobrolecki, S. S. Pathi, X. Y. Woo, K. C. Berrett, M. E. Wadsworth, J. H. Chuang, M. T. Lewis, G. T. Marth, J. Gertz, K. E. Varley, B. E. Welm and A. L. Welm, *Nat. Cancer*, 2022, **3**, 232–250.
3 X. Guan and S. Huang, *Front. Bioeng. Biotechnol.*, 2022, **10**, 1021966.
4 L. Meran, I. Massie, S. Campinoti, A. E. Weston, R. Gaifulina, L. Tullie, P. Faull, M. Orford, A. Kucharska, A. Baulies, L. Novellasdemunt, N. Angelis, E. Hirst, J. König, A. M. Tedeschi, A. F. Pellegata, S. Eli, A. P. Snijders, L. Collinson, N. Thapar, G. M. H. Thomas, S. Eaton, P. Bonfanti, P. De Coppi and V. S. W. Li, *Nat. Med.*, 2020, **26**, 1593–1601.
5 T. W. Dennison, R. D. Edgar, F. Payne, K. M. Nayak, A. D. B. Ross, A. Cenier, C. Glemas, F. Giachero, A. R. Foster, R. Harris, J. Kraiczy, C. Salvestrini, G. Stavrou, F. Torrente, K. Brook, C. Trayers, R. Elmentaite, G. Youssef, B. Tél, D. J. Winton, N. Skoufou-Papoutsaki, S. Adler, P. Bufler, A. Azabdaftari, A. Jenke, N. G, N. Thomas, E. Miele, A. Al-Mohammad, G. Guarda, S. Kugathasan, S. Venkateswaran, M. R. Clatworthy, T. Castro-Dopico, O. Suchanek, C. Strisciuglio, M. Gasparetto, S. Lee, X. Xu, E. Bello, N. Han, D. R. Zerbino, S. A. Teichmann, J. Nys, R. Heuschkel, F. Perrone and M. Zilbauer, *Gut*, 2024, **73**, 1464.
6 C. J. Childs, H. M. Poling, K. Chen, Y. H. Tsai, A. Wu, A. Vallie, M. K. Eiken, S. Huang, C. W. Sweet, R. Schreiner, Z. Xiao, R. C. Spencer, S. A. Paris, A. S. Conchola, J. W. Villanueva, M. F. Anderman, E. M. Holloway, A. Singh, R. J. Giger, M. M. Mahe, C. Loebel, M. A. Helmrath, K. D. Walton, S. Rafii and J. R. Spence, *Cell Stem Cell*, 2025, **32**, 640–651.
7 S. Reardon, *Nature*, 2017, DOI: **10.1038/nature.2017.21818**.
8 S. Chen, X. Chen, Z. Geng and J. Su, *Bioact. Mater.*, 2022, **18**, 15–25.
9 X. Qian, Y. Su, C. D. Adam, A. U. Deutschmann, S. R. Pather, E. M. Goldberg, K. Su, S. Li, L. Lu, F. Jacob, T. T. N. Phuong, S. Huh, A. Hoke, S. E. Swinford-Jackson, Z. Wen, X. Gu, R. C. Pierce, H. Wu, L. A. Briand, H. I. Chen, J. A. Wolf, H. Song and G. Ming, *Cell Stem Cell*, 2020, **26**, 766.
10 A. R. Abdel Fattah, S. Ghosh and I. K. Puri, *ACS Appl. Mater. Interfaces*, 2016, **8**, 11018–11023.
11 A. Purwada, M. K. Jaiswal, H. Ahn, T. Nojima, D. Kitamura, A. K. Gaharwar, L. Cerchietti and A. Singh, *Biomaterials*, 2015, **63**, 24–34.
12 D. Xie, B. Chen, W. Wang, W. Guo, Z. Sun, L. Wang, B. Shi, Y. Song and M. Su, *ACS Nano*, 2025, **19**, 12458–12466.

13 S. Lee, J. Kim, J. Seok, M. W. Kim, J. Rhee, G. Song, S. Park, S. Lee, Y. Jeong, H. M. Chung and C. Kim, *Biotechnol. J.*, 2024, **19**, 2300311.
14 Z. Peng, X. Lv, P. Zhang, Q. Chen, H. Zhang, J. Chen, X. Ma, B. Ouyang, M. Hao, H. Tong, D. Guo, Y. Luo and S. Huang, *Curr. Protein Pept. Sci.*, 2024, **25**, 71–82.
15 T. Thalheim, S. Siebert, M. Quaas, M. Herberg, M. R. Schweiger, G. Aust and J. Galle, *Cells*, 2021, **10**, 1718.
16 M. G. Andrews and A. R. Kriegstein, *Annu. Rev. Neurosci.*, 2022, **45**, 23–39.
17 N. Prior, P. Inacio and M. Huch, *Gut*, 2019, **68**, 2228–2237.
18 A. Bhaduri, M. G. Andrews, W. Mancia Leon, D. Jung, D. Shin, D. Allen, D. Jung, G. Schmunk, M. Haeussler, J. Salma, A. A. Pollen, T. J. Nowakowski and A. R. Kriegstein, *NATURE*, 2020, **578**, 142.
19 Y. Shi, X. Han, S. Zou and G. Liu, *ACS Nano*, 2024, **18**, 33276–33292.
20 G. R. Souza, J. R. Molina, R. M. Raphael, M. G. Ozawa, D. J. Stark, C. S. Levin, L. F. Bronk, J. S. Ananta, J. Mandelin, M. Georgescu, J. A. Bankson, J. G. Gelovani, T. C. Killian, W. Arap and R. Pasqualini, *Nat. Nanotechnol*, 2010, **5**, 291–296.
21 T. L. Li, Y. Liu, C. Forro, X. Yang, L. Beker, Z. Bao, B. Cui and S. P. Paşca, *Biomaterials*, 2022, **290**, 121825.
22 Y. Qin, B. Chen, Y. Hu, X. Zhang, Z. Wang, C. Ma, R. Yang, B. Wang, F. Li, S. Niu, Y. Han and D. Lu, *Adv. Healthcare Mater.*, 2025, **14**, e2404178.
23 R. Curvello and G. Garnier, *Biomacromolecules*, 2021, **22**, 701–709.
24 W. Ma, Y. Zheng, G. Yang, H. Zhang, M. Lu, H. Ma, C. Wu and H. Lu, *Mater. Horiz.*, 2024, **11**, 2957–2973.
25 A. Patino-Guerrero, H. Esmaeili, R. Q. Migrino and M. Nikkhah, *RSC Adv.*, 2023, **13**, 16985–17000.
26 D. J. Lomboni, A. Ozgun, T. V. de Medeiros, W. Staines, R. Naccache, J. Woulfe and F. Variola, *Adv. Healthcare Mater.*, 2024, **13**, e2301894.
27 Y. Tan, R. C. Coyle, R. W. Barrs, S. E. Silver, M. Li, D. J. Richards, Y. Lin, Y. Jiang, H. Wang, D. R. Menick, K. Deleon-Pennell, B. Tian and Y. Mei, *Sci. Adv.*, 2023, **9**, eadf2898.
28 Z. Luo, S. Zhang, J. Pan, R. Shi, H. Liu, Y. Lyu, X. Han, Y. Li, Y. Yang, Z. Xu, Y. Sui, E. Luo, Y. Zhang and S. Wei, *Biomaterials*, 2018, **163**, 25–42.
29 C. Afting, T. Walther, O. M. Drozdowski, C. Schlagheck, U. S. Schwarz, J. Wittbrodt and K. Göpfrich, *Nat. Nanotechnol*, 2024, **19**, 1849–1857.
30 H. L. Bumpers, D. G. Janagama, U. Manne, M. D. Basson and V. Katkoori, *J. Surg. Res.*, 2015, **194**, 319–326.
31 N. S. Lewis, E. E. Lewis, M. Mullin, H. Wheadon, M. J. Dalby and C. C. Berry, *J. Tissue Eng.*, 2017, **8**, 1545533460.
32 L. Labusca, D. D. Herea, A. E. Minuti, C. Stavila, C. Danceanu, M. Grigoras, G. Ababei, H. Chiriac and N. Lupu, *J. Biomed. Mater. Res., Part B*, 2021, **109**, 630–642.
33 W. R. Lee, K. T. Oh, S. Y. Park, N. Y. Yoo, Y. S. Ahn, D. H. Lee, Y. S. Youn, D. Lee, K. Cha and E. S. Lee, *Colloids Surf., B*, 2011, **85**, 379–384.
34 H. Tseng, A. C. Daquinag, G. R. Souza and M. G. Kolonin, *Methods Mol. Biol.*, 2018, **1773**, 147–154.
35 J. N. Ferreira, R. Hasan, G. Urkasemsin, K. K. Ng, C. Adine, S. Muthumariappan and G. R. Souza, *J. Tissue Eng. Regener. Med.*, 2019, **13**, 495–508.
36 I. Gaitán-Salvatella, E. O. López-Villegas, P. González-Alva, F. Susate-Olmos and M. A. Álvarez-Pérez, *Front. Mol. Biosci.*, 2021, **8**, 672518.
37 M. Urbanczyk, A. Zbinden, S. L. Layland, G. Duffy and K. Schenke-Layland, *Tissue Eng. Part A*, 2019, **26**, 387–399.
38 E. Barreto-Duran, C. C. Mejia-Cruz, L. F. Jaramillo-Garcia, E. Leal-Garcia, A. Barreto-Prieto and V. M. Rodriguez-Pardo, *J. Blood Med.*, 2021, **12**, 517–528.
39 L. A. Kotze, C. Beltran, D. Lang, A. G. Loxton, S. Cooper, M. Meiring, C. Koegelenberg, B. W. Allwood, S. T. Malherbe, A. M. Hiemstra, B. Glanzmann, C. Kinnear, G. Walzl and N. du Plessis, *mSphere*, 2021, **6**, e0055221.
40 L. Bonfim, P. de Queiroz Souza Passos, K. de Oliveira Gonçalves, L. C. Courrol, F. R. de Oliveira Silva and D. P. Vieira, *Appl. Nanosci.*, 2019, **9**, 1707–1717.
41 T. A. L. Brevini, E. F. M. Manzoni, S. Ledda and F. Gandolfi, in *Organoids: Stem Cells, Structure, and Function*, ed. K. Turksen, Springer New York, New York, NY, 2019, vol. 1576, pp. 291–299.
42 C. Frantz, K. M. Stewart and V. M. Weaver, *J. Cell Sci.*, 2010, **123**, 4195–4200.
43 X. Li, S. Sheng, G. Li, Y. Hu, F. Zhou, Z. Geng and J. Su, *Adv. Healthcare Mater.*, 2024, **13**, 2400431.
44 Z. Chen, H. Zhang, J. Huang, W. Weng, Z. Geng, M. Li and J. Su, *Mater. Today Bio*, 2025, **31**, 101509.
45 O. Y. Antonova, O. Y. Kochetkova, I. L. Kanev, E. A. Shlyapnikova and Y. M. Shlyapnikov, *ACS Chem. Neurosci.*, 2021, **12**, 2838–2850.
46 Y. You, F. Xu, L. Liu, S. Chen, Z. Ding and D. Sun, *Polymers*, 2024, **16**, 2664.
47 M. Beldjilali-Labro, R. Jellali, A. D. Brown, A. Garcia Garcia, A. Lerebours, E. Guenin, F. Bedoui, M. Dufresne, C. Stewart, J. Grosset and C. Legallais, in *International Journal of Molecular Sciences*, 2022, vol. 23, p. 260.
48 Z. Zhou, Y. Zhang, Y. Zeng, D. Yang, J. Mo, Z. Zheng, Y. Zhang, P. Xiao, X. Zhong and W. Yan, *ACS Nano*, 2024, **18**, 7688–7710.
49 A. A. Abdeen, J. Lee, N. A. Bharadwaj, R. H. Ewoldt and K. A. Kilian, *Adv. Healthcare Mater.*, 2016, **5**, 2536–2544.
50 Z. Zhang, S. Gao, Y. Hu, X. Chen, C. Cheng, X. Fu, S. Zhang, X. Wang, Y. Che, C. Zhang and R. Chai, *Adv. Sci.*, 2022, **9**, 2203557.
51 M. Bubna-Litic and R. Mayor, *Curr. Opin. Cell Biol.*, 2025, **94**, 102514.
52 C. Y. Shen, Q. R. Zhou, X. Wu, X. Y. Han, Q. Zhang, X. Chen, Y. X. Lai, L. Bai, Y. Y. Jing, J. H. Wang, C. L. Wang, Z. Geng and J. C. Su, *Mil. Med. Res.*, 2025, **12**, 39.
53 S. Fu, H. Li, Y. Wu and J. Wang, *J. Biomed. Mater. Res., Part A*, 2024, **112**, 193–209.
54 J. Dong and Q. Ma, *Nanotoxicology*, 2016, **10**, 699–709.

55 B. Sivaraman and A. Ramamurthi, *Acta Biomater.*, 2013, **9**, 6511–6525.
56 Q. Li, H. Lin, O. Wang, X. Qiu, S. Kidambi, L. P. Deleyrolle, B. A. Reynolds and Y. Lei, *Sci. Rep.*, 2016, **6**, 31915.
57 N. Gjorevski, N. Sachs, A. Manfrin, S. Giger, M. E. Bragina, P. Ordóñez-Morán, H. Clevers and M. P. Lutolf, *Nature*, 2016, **539**, 560–564.
58 F. A. Abdel and A. Ranga, *Front. Bioeng. Biotechnol.*, 2020, **8**, 240.
59 L. Bao, X. Cui, X. Wang, J. Wu, M. Guo, N. Yan and C. Chen, *ACS Nano*, 2021, **15**, 15858–15873.
60 A. M. Abdalla, T. Majdi, S. Ghosh and I. K. Puri, *Mater. Res. Express*, 2016, **3**, 125014.
61 I. C. Hou, L. Li, H. Zhang and P. Naumov, *Smart Mol.*, 2024, **16**(1), DOI: **10.1002/smo.20230031**.
62 D. Kokkinis, M. Schaffner and A. R. Studart, *Nat. Commun.*, 2015, **6**, 8643.
63 Y. Sapir-Lekhovitser, M. Y. Rotenberg, J. Jopp, G. Friedman, B. Polyak and S. Cohen, *Nanoscale*, 2016, **8**, 3386–3399.
64 M. Filippi, B. Dasen, J. Guerrero, F. Garello, G. Isu, G. Born, M. Ehrbar, I. Martin and A. Scherberich, *Biomaterials*, 2019, **223**, 119468.
65 H. Li, Y. Yin, Y. Xiang, H. Liu and R. Guo, *Biomed. Mater.*, 2020, **15**, 45004.
66 Q. Zhang, G. Yang, L. Xue, G. Dong, W. Su, M. J. Cui, Z. G. Wang, M. Liu, Z. Zhou and X. Zhang, *ACS Nano*, 2022, **16**, 21555–21564.
67 L. Ou, T. Wu, B. Qiu, H. Jin, F. Xu, H. Wu, W. Zhang, M. Xue, Z. Zhou, B. Lin, D. Sun and S. Chen, *ACS Appl. Mater. Interfaces*, 2024, **16**, 45861–45870.
68 Z. Lin, W. Wang, R. Liu, Q. Li, J. Lee, C. Hirschler and J. Liu, *Nat. Protoc.*, 2025, **20**, 2528–2559.
69 I. A. Marques, C. Fernandes, N. T. Tavares, A. S. Pires, A. M. Abrantes and M. F. Botelho, *Int. J. Mol. Sci.*, 2022, **23**, 12681.
70 J. A. Kim, J. Choi, M. Kim, W. J. Rhee, B. Son, H. Jung and T. H. Park, *Biomaterials*, 2013, **34**, 8555–8563.
71 H. Tseng, J. A. Gage, R. M. Raphael, R. H. Moore, T. C. Killian, K. J. Grande-Allen and G. R. Souza, *Tissue Eng., Part C*, 2013, **19**, 665–675.
72 P. Xiong, X. Huang, N. Ye, Q. Lu, G. Zhang, S. Peng, H. Wang and Y. Liu, *Adv. Sci.*, 2022, **9**, e2106049.
73 N. Li, X. Fan, K. Tang, X. Zheng, J. Liu and B. Wang, *Colloids Surf., B*, 2016, **140**, 287–296.
74 L. Rodriguez-Arco, I. A. Rodriguez, V. Carriel, A. B. Bonhome-Espinosa, F. Campos, P. Kuzhir, J. D. G. Duran and M. T. Lopez-Lopez, *Nanoscale*, 2016, **8**, 8138–8150.
75 C. Shen, Z. Zhang, X. Li, Y. Huang, Y. Wang, H. Zhou, L. Xiong, Y. Wen, H. Zou and Z. Liu, *Front. Immunol.*, 2023, **14**, 1172262.
76 E. Turker, N. Demircak and A. Arslan-Yildiz, *Biomater. Sci.*, 2018, **6**, 1996.
77 R. Onbas and A. Arslan Yildiz, *ACS Appl. Bio Mater.*, 2021, **4**, 1794–1802.
78 P. Krontiras, P. Gatenholm and D. A. Hägg, *J. Biomed. Mater. Res., Part B*, 2015, **103**, 195–203.
79 K. Markstedt, A. Mantas, I. Tournier, H. M. Avila, D. Hagg and P. Gatenholm, *Biomacromolecules*, 2015, **16**, 1489–1496.
80 D. A. Bowser and M. J. Moore, *Biofabrication*, 2020, **12**, 015002.
81 G. Urkasemsin, S. Rungarunlert and J. N. Ferreira, *Methods Mol. Biol.*, 2020, **2140**, 243–249.
82 J. Aalders, L. Leger, D. Piras, J. van Hengel and S. Ledda, *Methods Mol. Biol.*, 2021, **2273**, 85–102.
83 S. M. Park, S. J. Lee, J. Lim, B. C. Kim, S. J. Han and D. S. Kim, *ACS Appl. Mater. Interfaces*, 2018, **10**, 37878–37885.
84 G. Fang, Y. Chen, H. Lu and D. Jin, *Adv. Funct. Mater.*, 2023, **33**, 2215043.
85 N. Brandenberg, S. Hoehnel, F. Kuttler, K. Homicsko, C. Ceroni, T. Ringel, N. Gjorevski, G. Schwank, G. Coukos, G. Turcatti and M. P. Lutolf, *Nat. Biomed. Eng.*, 2020, **4**, 863.
86 G. Fang, H. Lu, A. Law, D. Gallego-Ortega, D. Jin and G. Lin, *Lab Chip*, 2019, **19**, 4093–4103.
87 D. Kim, K. Kim and J. Y. Park, *Lab Chip*, 2021, **21**, 1974–1986.
88 H. Shin, Y. Kook, H. J. Hong, Y. Kim, W. Koh and J. Lim, *Acta Biomater.*, 2016, **45**, 121–132.
89 H. Shin, H. J. Hong, W. Koh and J. Lim, *ACS Biomater. Sci. Eng.*, 2018, **4**, 4311–4320.
90 Y. Y. Choi, B. G. Chung, D. H. Lee, A. Khademhosseini, J. Kim and S. Lee, *Biomaterials*, 2010, **31**, 4296–4303.
91 D. Kim, S. J. Lee, J. Youn, H. Hong, S. Eom and D. S. Kim, *Biofabrication*, 2021, **13**, DOI: **10.1088/1758-5090/ac044c**.
92 F. Papes, A. P. Camargo, J. S. de Souza, V. Carvalho, R. A. Szeto, E. LaMontagne, J. R. Teixeira, S. H. Avansini, S. M. Sánchez-Sánchez, T. S. Nakahara, C. N. Santo, W. Wu, H. Yao, B. Araújo, P. Velho, G. G. Haddad and A. R. Muotri, *Nat. Commun.*, 2022, **13**, 2387.
93 Y. Liu, X. Xu, X. Ma, E. Martin-Rendon, S. Watt and Z. Cui, *Biotechnol. Prog.*, 2010, **26**(6), 1635–1643.
94 J. D. Finan and F. Guilak, *J. Cell. Biochem.*, 2010, **109**, 460–467.
95 Z. Han and J. C. Bishop, *CryoLetters*, 2020, **41**, 185–193.
96 H. Geng, X. Liu, G. Shi, G. Bai, J. Ma, J. Chen, Z. Wu, Y. Song, H. Fang and J. Wang, *Angew. Chem., Int. Ed.*, 2017, **56**, 997–1001.
97 R. Gao, W. Wang, Z. Wang, Y. Fan, L. Zhang, J. Sun, M. Hong, M. Pan, J. Wu, Q. Mei, Y. Wang, L. Qiao, J. Liu and F. Tong, *Adv. Healthcare Mater.*, 2024, **13**, 2401833.
98 W. Xue, H. Li, J. Xu, X. Yu, L. Liu, H. Liu, R. Zhao and Z. Shao, *Cells Rep. Methods*, 2024, **4**, 100777.
99 R. Dong, Y. Fei, Y. He, P. Gao, B. Zhang, M. Zhu, Z. Wang, L. Wu, S. Wu, X. Wang, J. Cai, Z. Chen and X. Zuo, *Adv. Sci.*, 2025, **12**, 2412559.
100 K. Saxena, S. E. Blutt, K. Ettayebi, X. Zeng, J. R. Broughman, S. E. Crawford, U. C. Karandikar, N. P. Sastri, M. E. Conner, A. R. Opekun, D. Y. Graham, W. Qureshi, V. Sherman, J. Foulke-Abel, J. In, O. Kovbasnjuk, N. C. Zachos, M. Donowitz and M. K. Estes, *J. Virol.*, 2015, **90**, 43–56.
101 V. Mangena, R. Chanoch-Myers, R. Sartore, B. Paulsen, S. Gritsch, H. Weisman, T. Hara, X. O. Breakefield,

K. Breyne, A. Regev, K. Chung, P. Arlotta, I. Tirosh and M. L. Suvà, *Cancer Discovery*, 2025, **15**, 299–315.
102 W. Shao, H. Xu, K. Zeng, M. Ye, R. Pei and K. Wang, *Stem Cell Res. Ther.*, 2025, **16**, 27.
103 M. M. A. Verstegen, F. J. M. Roos, K. Burka, H. Gehart, M. Jager, M. de Wolf, M. J. C. Bijvelds, H. R. de Jonge, A. I. Ardisasmita, N. A. van Huizen, H. P. Roest, J. de Jonge, M. Koch, F. Pampaloni, S. A. Fuchs, I. F. Schene, T. M. Luider, H. P. J. van der Doef, F. A. J. A. Bodewes, R. H. J. de Kleine, B. Spee, G. Kremers, H. Clevers, J. N. M. IJzermans, E. Cuppen and L. J. W. van der Laan, *Sci. Rep.*, 2020, **10**, 21900.
104 Z. Peng, X. Lv, H. Sun, L. Zhao and S. Huang, *Mol. Cancer*, 2025, **24**, 93.
105 D. Kharaghani, G. M. DeLoid, P. He, B. Swenor, T. H. Bui, N. Zuverza-Mena, C. Tamez, C. Musante, M. Verzi, J. C. White and P. Demokritou, *J. Hazard. Mater.*, 2025, **490**, 137714.
106 S. Yang, Y. Ge, T. Zhang, L. Yin, Y. Pu, Z. Chen and G. Liang, *Environ. Int.*, 2025, **195**, 109266.
107 P. Boix-Montesinos, P. Carrascosa-Marco, A. Armiñán and M. J. Vicent, *J. Controlled Release*, 2025, **381**, 113584.
108 D. Li and C. Liu, *Nat. Chem. Biol.*, 2021, **17**, 237–245.
109 J. Liang, D. Zhao, H. Yin, T. Tian, J. Kang, S. Shen and J. Wang, *Nano Today*, 2025, **61**, 102665.
110 S. Yui, T. Nakamura, T. Sato, Y. Nemoto, T. Mizutani, X. Zheng, S. Ichinose, T. Nagaishi, R. Okamoto, K. Tsuchiya, H. Clevers and M. Watanabe, *Nat. Med.*, 2012, **18**, 618–623.
111 A. Villaronga-Luque, R. G. Savill, N. López-Anguita, A. Bolondi, S. Garai, S. I. Gassaloglu, R. Rouatbi, K. Schmeisser, A. Poddar, L. Bauer, T. Alves, S. Traikov, J. Rodenfels, T. Chavakis, A. Bulut-Karslioglu and J. V. Veenvliet, *Cell Stem Cell*, 2025, **32**, 759–777.
112 X. Xu, Y. Liu and Z. Cui, *J. Tissue Eng. Regener. Med.*, 2014, **8**, 664–672.
113 M. J. Powell-Palm, V. Charwat, B. Charrez, B. Siemons, K. E. Healy and B. Rubinsky, *Commun. Biol.*, 2021, **4**, 1118.
114 D. Skubleny, S. Garg, J. Wickware, K. Purich, S. Ghosh, J. Spratlin, D. E. Schiller and G. R. Rayat, *Biomedicines*, 2023, **11**, 151.
115 G. D. Elliott, S. Wang and B. J. Fuller, *Cryobiology*, 2017, **76**, 74–91.
116 P. Kilbride, S. Lamb, S. Gibbons, J. Bundy, E. Erro, C. Selden, B. Fuller and J. Morris, *PLoS One*, 2017, **12**, e0183385.
117 N. Dolezalova, A. Gruszczyk, K. Barkan, J. A. Gamble, S. Galvin, T. Moreth, K. O'Holleran, K. T. Mahbubani, J. A. Higgins, F. M. Gribble, F. Reimann, J. Surmacki, S. Andrews, J. J. Casey, F. Pampaloni, M. P. Murphy, G. Ladds, N. Slater and K. Saeb-Parsy, *Sci. Rep.*, 2021, **11**, 10418.
118 K. Peter, M. Julie, M. C. Mira, R. Susan and C. Tessa, in *Cryopreservation*, ed. Q. Marian, IntechOpen, Rijeka, 2022, p. 5.
119 R. M. Warner, R. Shuttleworth, J. D. Benson, A. Eroglu and A. Z. Higgins, *Biophys. J.*, 2021, **120**, 4980–4991.
120 M. Wusteman, M. Robinson and D. Pegg, *Cryobiology*, 2004, **48**, 179–189.
121 G. J. Morris, M. Goodrich, E. Acton and F. Fonseca, *Cryobiology*, 2006, **52**, 323–334.
122 P. Kilbride and G. J. Morris, *Cryobiology*, 2017, **76**, 92–97.
123 S. Bojic, A. Murray, B. L. Bentley, R. Spindler, P. Pawlik, J. L. Cordeiro, R. Bauer and J. P. de Magalhães, *BMC Biol.*, 2021, **19**, 56.
124 Y. Diao, T. Hao, X. Liu and H. Yang, *Acta Biomater.*, 2024, **174**, 49–68.
125 K. A. Murray, Y. Gao, C. A. Griffiths, N. Kinney, Q. Guo, M. I. Gibson and T. F. Whale, *JACS Au*, 2023, **3**, 1314–1320.
126 M. L. Etheridge, Y. Xu, L. Rott, J. Choi, B. Glasmacher and J. C. Bischof, *Technology*, 2014, **02**, 229–242.
127 A. Lawson, I. N. Mukherjee and A. Sambanis, *Cryobiology*, 2012, **64**, 1–11.
128 A. Abazari, N. M. Jomha, J. A. W. Elliott and L. E. McGann, *Cryobiology*, 2013, **66**, 201–209.
129 A. M. Vian and A. Z. Higgins, *Cryobiology*, 2014, **68**, 35–42.
130 A. Fatehullah, S. H. Tan and N. Barker, *Nat. Cell Biol.*, 2016, **18**, 246–254.
131 J. Tan, J. Li, C. Lin, N. Ye, H. Zhang, C. Liu, S. Han, Z. Li and X. Zhou, *Life Sci.*, 2024, **355**, 122980.
132 T. F. Zur Bruegge, A. Liese, S. Donath, S. Kalies, M. Kosanke, O. Dittrich-Breiholz, S. Czech, V. N. Bauer, A. Bleich and M. Buettner, *Stem Cells Int.*, 2021, **2021**, 9041423.
133 Q. Liu, T. Zhao, X. Wang, Z. Chen, Y. Hu and X. Chen, *Micromachines*, 2021, **12**, 624.
134 Y. K. Chong, T. B. Toh, N. Zaiden, A. Poonepalli, S. H. Leong, C. E. Ong, Y. Yu, P. B. Tan, S. J. See, W. H. Ng, I. Ng, M. P. Hande, O. L. Kon, B. T. Ang and C. Tang, *Stem Cells*, 2009, **27**, 29–39.
135 U. A. Okoli, M. T. Okafor, K. A. Agu, A. C. Ndubuisi, I. J. Nwigwe, E. O. Nna, O. C. Okafor, F. I. Ukekwe, T. U. Nwagha, V. C. Menkiti, C. O. Eze, K. C. Onyekwelu, J. E. Ikekpeazu, C. A. Anusiem, A. U. Mbah, C. P. Chijioke and I. J. Udeniya, *Cryobiology*, 2020, **97**, 179–184.
136 R. E. Thompson, M. A. Meyers, C. Premanandan and F. K. Hollinshead, *Theriogenology*, 2023, **196**, 167–173.
137 Z. Liu, X. Zheng and J. Wang, *J. Am. Chem. Soc.*, 2022, **144**, 5685–5701.
138 H. Dong, X. Li, K. Chen, N. Li and H. Kagami, *Tissue Eng., Part C*, 2021, **27**, 253–263.
139 D. Kaiser, N. M. Otto, O. McCallion, H. Hoffmann, G. Zarrinrad, M. Stein, C. Beier, I. Matz, M. Herschel, J. Hester, G. Moll, F. Issa, P. Reinke and A. Roemhild, *Front. Cell Dev. Biol.*, 2021, **9**, 750286.
140 D. Diaz-Dussan, Y. Peng, J. Sengupta, R. Zabludowski, M. K. Adam, J. P. Acker, R. N. Ben, P. Kumar and R. Narain, *Biomacromolecules*, 2020, **21**, 1264–1273.
141 R. Li, K. Hornberger, J. R. Dutton and A. Hubel, *Front. Bioeng. Biotechnol.*, 2020, **8**, 1.
142 T. F. Whale, M. Rosillo-Lopez, B. J. Murray and C. G. Salzmann, *J. Phys. Chem. Lett.*, 2015, **6**, 3012–3016.
143 Y. Hou, X. Sun, M. Dou, C. Lu, J. Liu and W. Rao, *Nano Lett.*, 2021, **21**, 4868–4877.

144 W. Han, L. Zhong, J. Zhang, Y. Li, N. Li, Z. Wang and J. Zhao, *ACS Appl. Nano Mater.*, 2024, **7**, 12783–12794.
145 Q. Lei, Y. Sun, J. Huang, W. Liu, X. Zhan, W. Yin, S. Guo, A. Sinelshchikova, C. J. Brinker, Z. He, J. Guo, S. Wuttke and W. Zhu, *Angew. Chem., Int. Ed.*, 2023, **62**, e202217374.
146 S. Ding, S. Ali, S. Zhang, J. Zhao, C. Liu, M. A. Aslam, X. Yu, M. Xi, L. Pan, N. Li and Z. Wang, *ACS Omega*, 2023, **8**, 10466–10475.
147 M. Stefanic, K. Ward, H. Tawfik, R. Seemann, V. Baulin, Y. Guo, J. Fleury and C. Drouet, *Biomaterials*, 2017, **140**, 138–149.
148 W. Rao, H. Huang, H. Wang, S. Zhao, J. Dumbleton, G. Zhao and X. He, *ACS Appl. Mater. Interfaces*, 2015, **7**, 5017–5028.
149 Y. Zhang, H. Wang, S. Stewart, B. Jiang, W. Ou, G. Zhao and X. He, *Nano Lett.*, 2019, **19**, 9051–9061.
150 X. Yao, J. J. Jovevski, M. F. Todd, R. Xu, Y. Li, J. Wang and S. Matosevic, *Adv. Sci.*, 2020, **7**, 1902938.
151 A. Maruf, M. Milewska, K. Dudzisz, A. Lalik, S. Student, A. Salvati and I. Wandzik, *Biomacromolecules*, 2025, **26**, 2835–2851.
152 Y. Cao, M. Hassan, Y. Cheng, Z. Chen, M. Wang, X. Zhang, Z. Haider and G. Zhao, *ACS Appl. Mater. Interfaces*, 2019, **11**, 12379–12388.
153 G. Bai, Z. Song, H. Geng, D. Gao, K. Liu, S. Wu, W. Rao, L. Guo and J. Wang, *Adv. Mater.*, 2017, **29**, 1606843.
154 C. Cline, H. Wang, J. Kong, T. Li, J. Liu and U. Wegst, *Langmuir*, 2022, **38**, 15121–15131.
155 Z. Wang, B. Yang, Z. Chen, D. Liu, L. Jing, C. Gao, J. Li, Z. He and J. Wang, *ACS Appl. Bio Mater.*, 2020, **3**, 3785–3791.
156 F. Baniasadi, S. Hajiaghalou, A. Shahverdi, M. R. Ghalamboran, V. Pirhajati and R. Fathi, *Reprod. Sci.*, 2023, **30**, 2122–2136.
157 Y. Cao, T. Chang, C. Fang, Y. Zhang, H. Liu and G. Zhao, *ACS Nano*, 2022, **16**, 8837–8850.
158 W. Zhu, J. Guo, J. O. Agola, J. G. Croissant, Z. Wang, J. Shang, E. Coker, B. Motevalli, A. Zimpel, S. Wuttke and C. J. Brinker, *J. Am. Chem. Soc.*, 2019, **141**, 7789–7796.
159 P. Zhang, R. Zou, S. Wu, L. Meyer, J. Wang and T. Kraus, *Langmuir*, 2022, **38**, 2460–2466.
160 N. Jeon, I. Choi, P. C. W. Lee and E. Lee, *ACS Appl. Nano Mater.*, 2022, **5**, 15418–15428.
161 S. Liu, Z. Han, Z. Ye, M. Jiang, M. L. Etheridge, J. C. Bischof and Y. Yin, *Nano Lett.*, 2024, **24**, 11567–11572.
162 D. E. Mitchell, J. R. Lovett, S. P. Armes and M. I. Gibson, *Angew. Chem., Int. Ed.*, 2016, **55**, 2801–2804.
163 P. G. Georgiou, I. Kontopoulou, T. R. Congdon and M. I. Gibson, *Mater. Horiz.*, 2020, **7**, 1883–1887.
164 R. Gao, W. Wang, Z. Wang, Y. Fan, L. Zhang, J. Sun, M. Hong, M. Pan, J. Wu, Q. Mei, Y. Wang, L. Qiao, J. Liu and F. Tong, *Adv. Healthcare Mater.*, 2024, **13**, e2401833.
165 L. E. Ehrlich, Z. Gao, J. C. Bischof and Y. Rabin, *PLoS One*, 2020, **15**, e0238941.
166 M. E. Mamprin, E. E. Guibert and J. V. Rodriguez, *Cryobiology*, 2000, **40**, 270–276.
167 K. Benhenia, H. Rahab, M. A. Smadi, H. Benmakhlouf, A. Lamara, T. Idres and M. Iguer-Ouada, *Anim. Reprod. Sci.*, 2018, **195**, 266–273.
168 J. P. Morrow, D. Pizzi, Z. A. I. Mazrad, A. I. Bush and K. Kempe, *Biomater. Sci.*, 2023, **11**, 3159–3171.
169 A. A. Timralieva, I. V. Moskalenko, P. V. Nesterov, V. V. Shilovskikh, A. S. Novikov, E. A. Konstantinova, A. I. Kokorin and E. V. Skorb, *ACS Omega*, 2023, **8**, 8276–8284.
170 T. Shimizu, R. Kishi, T. Yamada and K. Hata, *RSC Adv.*, 2020, **10**, 29419–29423.
171 L. Rodriguez-Arco, I. A. Rodriguez, V. Carriel, A. B. Bonhome-Espinosa, F. Campos, P. Kuzhir, J. D. G. Duran and M. T. Lopez-Lopez, *Nanoscale*, 2016, **8**, 8138–8150.
172 W. A. Khalil, M. A. El-Harairy, A. E. B. Zeidan and M. A. E. Hassan, *Theriogenology*, 2019, **126**, 121–127.
173 J. H. Crowe, L. M. Crowe, W. F. Wolkers, A. E. Oliver, X. Ma, J. Auh, M. Tang, S. Zhu, J. Norris and F. Tablin, *Integr. Comp. Biol.*, 2005, **45**, 810–820.
174 M. Wang, B. Zhang, C. Chen, Q. Gao, P. Zhou and G. Zhao, *Langmuir*, 2025, **41**, 12264–12275.
175 D. S. Moore and S. C. Hand, *Cryobiology*, 2016, **73**, 240–247.
176 T. Uchida, M. Furukawa, T. Kikawada, K. Yamazaki and K. Gohara, *Cryobiology*, 2017, **77**, 50–57.
177 Y. Hu, X. Liu, F. Liu, J. Xie, Q. Zhu and S. Tan, *ACS Biomater. Sci. Eng.*, 2023, **9**, 1190–1204.
178 W. Zhang, J. Rong, Q. Wang and X. He, *Nanotechnology*, 2009, **20**, 275101.
179 M. Xu, Y. Song, J. Zhang, Y. Zhao, H. Geng, X. Weng, Z. Liu, J. Cheng and T. Yan, *Chin. J. Biotechnol.*, 2024, **40**, 2294–2307.
180 K. A. Murray, Y. Gao, C. A. Griffiths, N. Kinney, Q. Guo, M. I. Gibson and T. F. Whale, *JACS Au*, 2023, **3**, 1314–1320.
181 N. G. Lamson, A. Berger, K. C. Fein and K. A. Whitehead, *Nat. Biomed. Eng.*, 2020, **4**, 84–96.
182 H. Ruan, T. Wang and C. Gao, *CryoLetters*, 2020, **41**, 26–30.
183 Y. XU, N. GUO, G. YANG, T. ZHAN, H. HAN, Y. CHENG, G. ZHAO, Q. WEI, X. ZHOU and B. LIU, *Sci. Sin. Vitae*, 2023, **53**, 1021–1034.
184 R. Chen, B. Wang, Y. Liu, R. Lin, J. He and D. Li, *Cryobiology*, 2018, **82**, 1–7.
185 L. Eini, M. Naseri, F. Karimi-Busheri, M. Bozorgmehr, R. Ghods and Z. Madjd, *J. Cell. Physiol.*, 2020, **235**, 2452–2463.
186 G. Dunaevskiy, E. Gavrilin, A. Pomytkin, R. Sorokin, A. Kuznetsov, V. Antipov and A. Nechaev, *Sci. Rep.*, 2023, **13**, 1362.
187 L. Cirino, S. Tsai, L. Wang, C. Chen, W. Hsieh, C. Huang, Z. Wen and C. Lin, *Cryobiology*, 2021, **98**, 80–86.
188 N. E. Estrin, A. Lesniewski, S. McClain, W. Hou and G. E. Romanos, *Photobiomodulation, Photomed., Laser Surg.*, 2022, **40**, 410–416.
189 Y. Hou, C. Lu, M. Dou, C. Zhang, H. Chang, J. Liu and W. Rao, *Acta Biomater.*, 2020, **102**, 403–415.

190 C. Alvarez, C. Berrospe-Rodriguez, C. Wu, J. Pasek-Allen, K. Khosla, J. Bischof, L. Mangolini and G. Aguilar, *Front. Bioeng. Biotechnol.*, 2022, **10**, 957481.
191 A. Chiu-Lam and C. Rinaldi, *Adv. Funct. Mater.*, 2016, **26**, 3933–3941.
192 J. Wang, G. Zhao, Z. Zhang, X. Xu and X. He, *Acta Biomater.*, 2016, **33**, 264–274.
193 M. L. Etheridge, Y. Xu, J. Choi and J. C. Bischof, *Cryobiology*, 2013, **67**, 398–399.
194 T. Wakabayashi, M. Kaneko, T. Nakai, M. Horie, H. Fujimoto, M. Takahashi, S. Tanoue and A. Ito, *Bioeng. Transl. Med.*, 2022, **8**, e10416.
195 P. Singh, K. Duraisamy, C. Raitmayr, K. S. Sharma, T. Korzun, K. Singh, A. S. Moses, K. Yamada, V. Grigoriev, A. A. Demessie, Y. Park, Y. T. Goo, B. Mamnoon, A. P. M. Souza, K. Michimoto, K. Farsad, A. Jaiswal, O. R. Taratula and O. Taratula, *Adv. Funct. Mater.*, 2025, **35**, 2414719.
196 Z. Ye, S. Liu and Y. Yin, *Mater. Chem. Front.*, 2023, **7**, 3427–3433.
197 P. Joshi and Y. Rabin, *PLoS One*, 2023, **18**, e0290063.
198 N. Manuchehrabadi, Z. Gao, J. Zhang, H. L. Ring, Q. Shao, F. Liu, M. McDermott, A. Fok, Y. Rabin, K. G. M. Brockbank, M. Garwood, C. L. Haynes and J. C. Bischof, *Sci. Transl. Med.*, 2017, **9**, eaah4586.
199 S. Karimi, S. N. Tabatabaei, M. G. Novin, M. Kazemi, Z. S. Mofarahe and A. Ebrahimzadeh-Bideskan, *Heliyon*, 2023, **9**, e18828.
200 D. Ivanov, A. Hoeppel, T. Weigel, R. Ossikovski, S. Dembski and T. Novikova, in *Photonics*, 2023, vol. 10.
201 X. Liu, G. Zhao, Z. Chen, F. Panhwar and X. He, *ACS Appl. Mater. Interfaces*, 2018, **10**, 16822–16835.
202 H. L. Ring, Z. Gao, A. Sharma, Z. Han, C. Lee, K. G. M. Brockbank, E. D. Greene, K. L. Helke, Z. Chen, L. H. Campbell, B. Weegman, M. Davis, M. Taylor, S. Giwa, G. M. Fahy, B. Wowk, R. Pagotan, J. C. Bischof and M. Garwood, *Magn. Reson. Med.*, 2020, **83**, 1750–1759.